Journal of Hydrology 414–415 (2012) 435–451

Contents lists available at SciVerse ScienceDirect

Journal of Hydrology

journal homepage: www.elsevier.com/locate/jhydrol

Assessment of the impact of anthropogenic activities on the groundwater hydrology and chemistry in Tarsus coastal plain (Mersin, SE Turkey) using fuzzy clustering, multivariate statistics and GIS techniques

Cüneyt Güler *, Mehmet Ali Kurt, Musa Alpaslan, Can Akbulut

Mersin Üniversitesi, Çiftlikköy Kampüsü, Jeoloji Mühendisliği Bölümü, 33343 Mersin, Turkey

ARTICLE INFO

Article history:
Received 17 January 2011
Received in revised form 29 September 2011
Accepted 9 November 2011
Available online 18 November 2011
This manuscript was handled by Laurent Charlet, Editor-in-Chief, with the assistance of Jose D. Salas, Associate Editor

Keywords:
Coastal aquifer
Fuzzy *c*-means clustering
Principal components analysis
Geographic information systems
Salinization
PHREEQC

SUMMARY

Tarsus coastal plain (TCP) is an economically and ecologically important area situated in between the fertile fluvio-deltaic plains of two rivers, Deliçay and Tarsus (Mersin, SE Turkey), where anthropogenic activities (agricultural, industrial, and domestic) are very intense. Twenty-four water quality parameters were surveyed at 193 groundwater and 10 surface water sites during August 2008. The objective was to characterize the physico-chemical properties of groundwaters in TCP, assess the impact of anthropogenic activities on the groundwater hydrology and chemistry, and identify the major hydrogeochemical processes occurring in the area. Groundwater samples were grouped into hydrochemically distinct and spatially continuous four water classes (i.e., C1, C2, C3, and C4) using the fuzzy *c*-means (FCM) clustering method, where membership values were interpolated using the ordinary kriging technique. Principal components analysis (PCA) was used to decipher various underlying natural and anthropogenic processes creating these distinct water classes. Four principal components (PCs) were extracted in PCA which explained more than 73% of the total variance in water quality. Major factors responsible for the variations in chemistries of water classes are identified as: (1) water–rock interaction and nitrate contamination; (2) salinization by seawater intrusion and evaporite dissolution; (3) geogenic/anthropogenic Cr, Fe, and Mn; and (4) anthropogenic Zn pollution. Overexploitation of the aquifer is clearly evident, especially at settlements located near the coastal zone, where the water table is lowered 2–5 m below the sea level. Salinization is well known in the area and is attributed not only to seawater intrusion, but also to dissolution of evaporitic series from the Handere formation. Hydrochemical evidence also suggest that in the area subsurface paleo-river channels and the deposits infilling the ancient lagoon area within Quaternary–Recent alluvial deposits act as significant hydrological features where preferential groundwater flow occurs along them.

1. Introduction

In both inland and coastal areas of Turkey, groundwater resources play an increasingly vital role in supply of potable water as population continues to grow steadily. Nevertheless, nationwide monitoring studies conducted by the government agencies (i.e., Baltacı et al., 2008) raise concern over an increasing trend for deterioration in quality of water supplies mainly due to anthropogenic activities. Moreover, in the forthcoming decade, the climate change is projected to exacerbate the pressure on the hydrologic system (especially in the Mediterranean region), along with the natural habitats associated with it (Ministry of Environment and Forestry, 2009). This situation calls for an urgent need for an effective strategy to reduce the pressure on the hydrologic system, including both its living and non-living components. Contrary to common belief, groundwater and associated hyporheic zones is not completely devoid of life, but support diverse subsurface fauna and microbiota (Hancock et al., 2005 and references therein) that are responsible for a myriad of (bio)geochemical reactions, imperative for a fully functioning system. It is also known that even minute changes in the chemical characteristics of groundwater can broadly disrupt many important ecological processes (Moore, 1999; Murgai et al., 2001). Therefore, sustainable management of groundwater resources requires a good understanding of both groundwater circulation patterns and hydrologic/hydrochemical processes that affect their chemistry, in order to ensure a reliable supply for all life forms.

In Mersin province (2009 population > 1,640,000) of Turkey, the majority of dense human settlements are generally confined to narrow coastal strips or to relatively wide and flat-lying delta areas located between the Taurus Mountains and Mediterranean Sea. Since the historical periods, nearly flat topography combined with a mild climate made these coastal areas very attractive for human inhabitation and a variety of land uses. Being fed by four major

* Corresponding author. Tel.: +90 324 361 0001x7314; fax: +90 324 361 0032.
E-mail address: cuneytguler@gmail.com (C. Güler).

0022-1694/$ - see front matter © 2011 Elsevier B.V. All rights reserved.
doi:10.1016/j.jhydrol.2011.11.021

perennial rivers (Göksu, Lamas, Tarsus, and Seyhan) and numerous ephemeral streams originating from the Taurus Mountains, the delta areas have abundance of water that supports terrestrial, limnic, and marine ecosystems of international importance (Yılmaz, 1998). Tarsus coastal plain (TCP) is one of the most important one of these coastal environments and provides space not only for delicate natural habitats but also for agriculture, heavy industry, settlement, as well as transportation (Fig. 1). However, due to rapid industrial growth (Güler, 2009), unplanned urbanization, land use/land cover (LULC) changes (including modification of the drainage patterns and basin hydrology) (Gürbüz, 1999; Sandal and Gürbüz, 2003), excessive use of synthetic chemicals in agriculture (Kumbur et al., 2008), together with overexploitation of the coastal aquifers (Demirel, 2004) have collectively resulted in qualitative and quantitative degradation of the groundwater resources in TCP. The lack of basin-wide management strategies and occurrence of pollution from various point and diffuse sources only add complexity of the problem. The current situation exerts a huge pressure on the TCP ecosystem resulting in loss of critical habitats, decrease in biodiversity (MEDASSET, 2001, 2009), and degradation of water/soil quality in the area (Yılmaz et al., 1998; Demirel, 2004; Koleli and Halisdemir, 2005; Çelik et al., 2006). Such a situation necessitates comprehensive studies that will characterize and diagnose the present condition of this coastal environment.

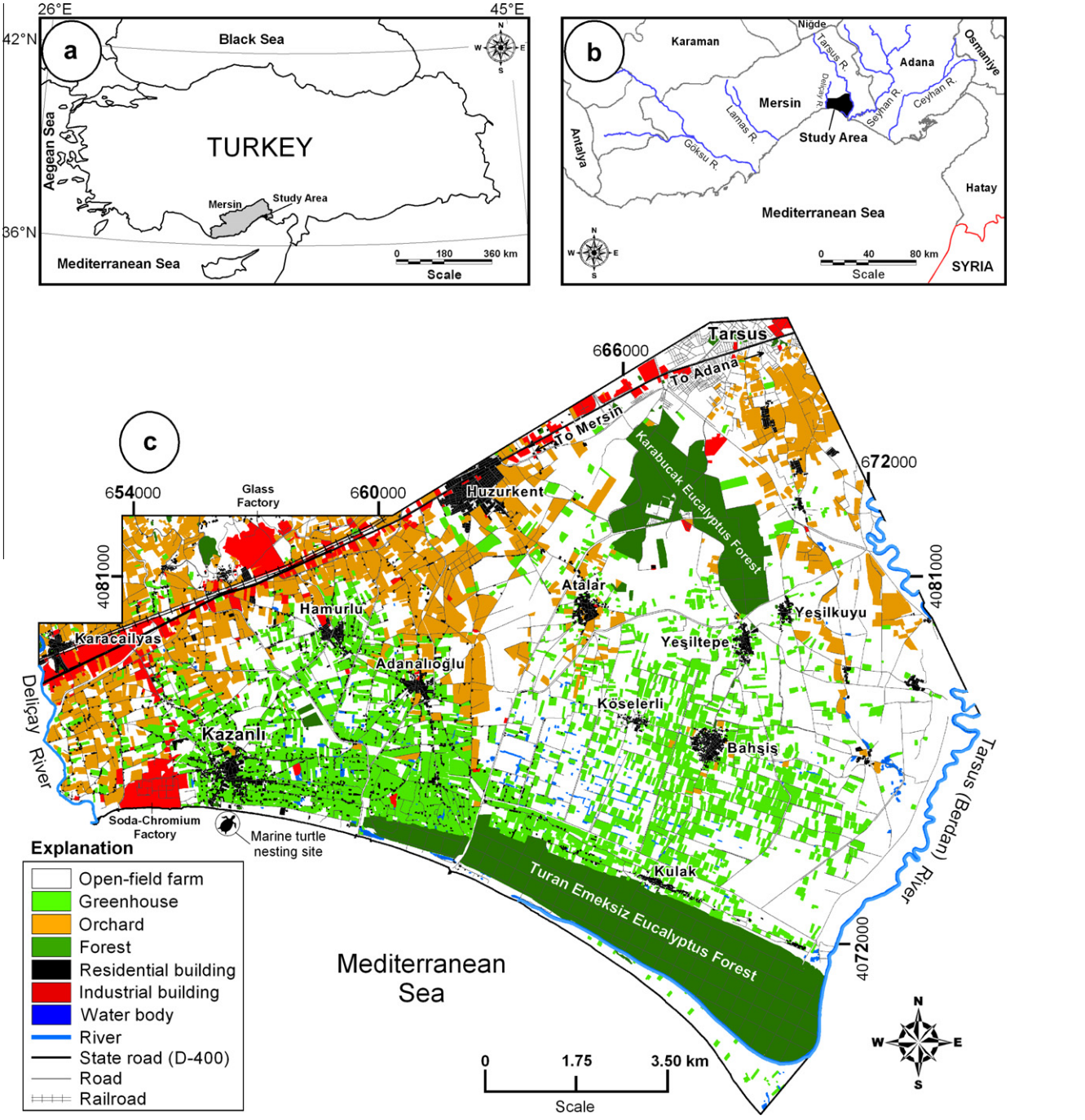

Fig. 1. (a) Location of the Mersin province within the Turkey, (b) detailed map showing the Tarsus coastal plain (TCP) area and major perennial rivers draining to the Mediterranean Sea, and (c) land use/land cover (LULC) map of the TCP (digitized from Quickbird satellite images acquired in 2004).

However, this is not an easy task due to natural gradients and ongoing changes occurring as a result of the intense anthropogenic activities.

In hydrologic systems, often the physico-chemical properties of groundwater show a gradual change (both in geographical and data space) along the flow path (Güler and Thyne, 2004), rather than forming discrete entities delineated by sharp boundaries (Güler et al., 2002). This limits the efficacy of the rigid statistical clustering techniques (e.g., hard *k*-means) for hydrochemical data classification, because near the class boundaries samples generally display a transitional character in chemistry, hence they are susceptible to misclassification (Güler and Thyne, 2004). Methods related to "fuzzy logic" may be best suited for that purpose since they can provide extra information about the membership degrees of the water samples in a class. Fuzzy (i.e., soft) clustering techniques (i.e., FCM) have already been successfully applied in several studies to detect changes in water quality parameters and partition samples into homogeneous and continuous classes (Barbieri et al., 2001; Güler et al., 2002; Güler and Thyne, 2004). Since water samples and their physico-chemical attributes are geographic entities in nature, application of fuzzy clustering together with geographic information systems (GISs) and statistical/geostatistical tools is a logical combination that can assist us to elucidate the hidden patterns in the data and provide an opportunity for an in-depth assessment of the current state of the site. In this study, a rigorous treatise on groundwater chemistry is provided to close the information gap regarding the hydrochemical processes occurring in the area and the impact of anthropogenic activities on the groundwater hydrology and chemistry. In this paper, the focus is set on fuzzy *c*-means (FCM) clustering of the groundwater samples into homogenous and continuous classes that may reflect various underlying hydrologic and/or hydrochemical processes. Additionally, principal components analysis (PCA) was used to reduce the dimensions of the available data and to decipher the underlying factors affecting the groundwater quality in the area. The chemistry of groundwater was also compared with that of surface waters from the area to gain a better understanding on interactions occurring between them. In this study, GIS and spatial interpolation techniques were used for data integration, retrieval, analysis and visualization of the study findings.

2. Description of the study area

2.1. Geographic location, land use, and climate

The TCP area stretches from Deliçay River on the west to Tarsus (Berdan) River on the east and is located between the Mersin–Tarsus segment of the state road D-400 and the Mediterranean Sea, covering an area of 234 km^2 (Fig. 1). There are several small villages and towns scattered throughout the area with a total population about 44,000; excluding the city of Tarsus, which has a population of nearly 228,500 (2008 census). Currently, agricultural crop production and a variety of industrial investments located along the coastline constitute the most important economic activities in TCP. In modern terms, industrialization in the area dates back to the early 1950s with the establishment of ATAŞ petroleum refinery in Karaduvar (near Deliçay River) (Güler, 2009). From the mid-1960s onwards, the area rapidly became a major attraction center for a wide variety of industry mainly because of its proximity to the Mersin International Port (~5 km to the west) and Mersin–Tarsus–Adana road/railroad. There are six key industrial economic sectors in the region including production of heavy machinery and spare parts, textiles, building materials (cement, plaster, brick, glass, and ceramics), chemicals (sodium/chromium products and plastics), food/fruit processing, and storage facilities for refined petroleum products.

Table 1
Land use/land cover (LULC) details of the Tarsus coastal plain.

Land use class	Area (km^2)	Percentage of total area (%)
Open-field farm	138.15	59.04
Greenhouse	31.53	13.47
Orchard (citrus)	27.05	11.56
Forest (eucalyptus)	25.99	11.11
Industrial	6.64	2.84
Residential	3.76	1.60
Water bodies	0.88	0.38
Total area	234	100

Based on the data obtained from supervised classification of Quickbird satellite images (acquired on 2004), land use in the area has a complex pattern, where most of the area (~84%) is devoted to agricultural activities (Fig. 1 and Table 1). The majority of the remaining area can be classified as forest (i.e., eucalyptus), industrial, and residential. In the area, topographic gradients are generally low, ranging from 0.1% or less in the southern parts to 8% in the northeast (near the city of Tarsus). The elevations are between 0 and 30 m above mean sea level (MSL) and display an undulating topography, which is particularly characteristic for the sand dune areas along the coast.

The climate in TCP is typically Mediterranean, characterized by hot and dry summers, and relatively mild and rainy winters. In the coastal part, mean annual temperature is around 18 °C. Temperatures occasionally rise above 30 °C in summer and rarely fall below 5 °C in winter (Kafalı Yılmaz, 2008). However, alpine climate conditions prevail in the northern part, in the Taurus Mountains. In TCP, average annual rainfall is 609.5 mm, of which 77.7% occurs between November and March (Gürses, 1995). Whereas, average annual potential evapotranspiration reaches 968 mm and around 81% of it occurs between May and October (Kafalı Yılmaz, 2008). Dominant winds in the area are generally north-easterly and carry coastal sands and sea spray inland. The total surface runoff from the mountains at north is about 44 m^3 s^{-1} via Deliçay and Tarsus rivers, the latter accounting for almost 95% of this amount (Ministry of Environment and Forestry, 2008).

2.2. Environmental implications of the historic and current human activities in the TCP

Historically, Tarsus was an important settlement since Neolithic times (Goldman, 1956) and a focal point of many civilizations including the ancient Romans when it was the capital of the Cilicia province (Goldman, 1950). During those times, Tarsus was a port city, where the Tarsus River flowed through it and then poured into a lagoon named Rhegma (which provided the city's link to the sea and served as a natural harbor) (Fant and Reddish, 2003). In the 6th century, a major portion of the flow in the river was diverted to a new channel by the Byzantine emperor Justinian I (527–565 A.D.) with an intention to carry off the excess waters in time of flood (Zoroğlu, 1995). Nevertheless, alluvial material brought down throughout centuries by the river, together with windblown sands from the coastal part, filled up the old river channel and the Rhegma lagoon by the 19th century (Göney, 1976; Öner et al., 2005). Later, the area became a marshland called Aynaz (Fig. 2). Today, the city of Tarsus has no longer access to the sea and lies nearly 16 km inland. During the past century, especially between 1900s and 1960s, extensive efforts have been devoted by the government to reclaim the marshland areas (Yılmaz, 1998). These efforts have included planting exotic tree species (i.e., *Eucalyptus camaldulensis*) over large areas, laying a dense network of drainage canals, drilling pumping wells and building flood walls and dams to lower the groundwater levels (Fig. 2). For instance, the Tarsus River was

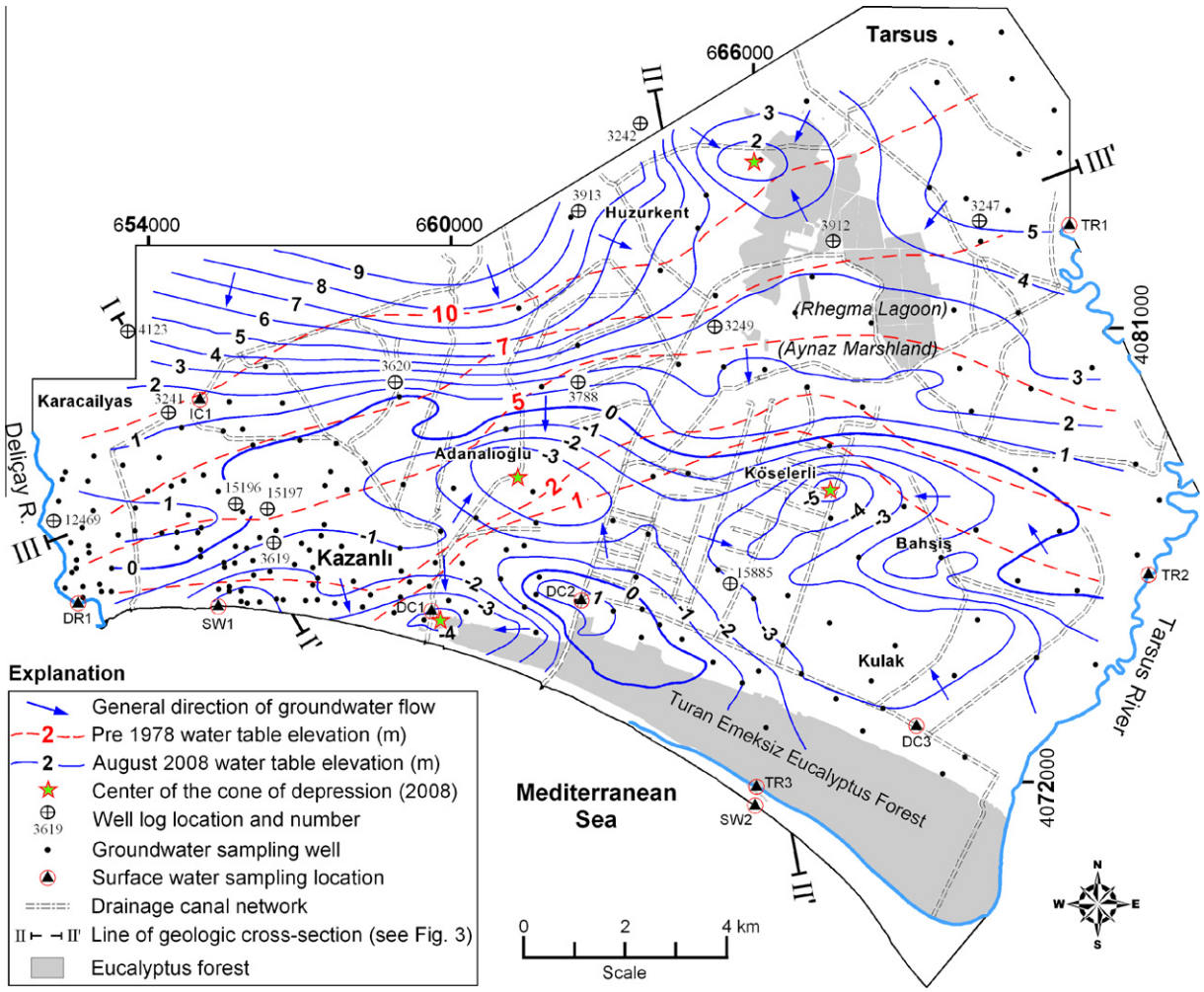

Fig. 2. Map showing the locations of groundwater (n = 193) and surface water (n = 10) sampling sites and the water table elevations (pre 1978 and 2008) in the Tarsus coastal aquifer. Water table elevations are in meters above mean sea level. Pre 1978 water level contours were digitized from DSİ (1978). Arrows depict the groundwater flow directions. Drainage canal network and the boundary of eucalyptus forests were digitized from Quickbird satellite images acquired in 2004.

dammed in 1902 to build Turkey's first micro-scale hydroelectric power plant (Öztürk, 2004). All these efforts have resulted in a sharp decline in the groundwater levels throughout the area and subsequent drainage of the marshland areas, including the Aynaz. After completion of the Berdan irrigation/drainage canal projects in 1960s and the Berdan dam in 1984, agricultural activities in the area have been intensified, especially in citrus fruit production (Sandal and Gürbüz, 2003). Fertile alluvial soils and climate conditions favor cropping throughout the year (2–3 times) and planting of a wide variety of crop species including cereals, grapes, vegetables, and salad herbs (Sandal and Gürbüz, 2003). Since the last three decades; however, agricultural areas have been markedly decreasing due to industrial and urban expansions.

The ecological importance of the TCP, on the other hand, can be attributed to the existence of delicate coastal ecosystems. This area hosts one of the largest coastal dune areas in Turkey (Uslu, 1989). Unfortunately, coastal dunes are seriously threatened by several factors including coastal erosion (MEDASSET, 2009), excessive sand extraction (Yılmaz, 1998), spread of greenhouses, and construction of large dams on the rivers supplying alluvial material to the delta (Gürbüz, 1999, 2003). Protection of the coastal dune areas is crucial because 4.5-km beach at Kazanlı (Fig. 1) is the second most important nesting site in the Mediterranean for the "critically endangered" marine turtle species such as the *Chelonia mydas* and *Caretta caretta* (Canbolat, 2004). These marine turtle species are protected under the Bern and CITES conventions (IUCN, 2007). Nevertheless, a recent study conducted by Çelik et al. (2006) on terrestrial and marine plant/sediment samples collected from the nesting grounds has shown very high levels of several trace elements (e.g., Cd, Cr, and Pb). Additionally, marine turtle carcasses found on the Kazanlı beach (Kaska et al., 2004) and marine bivalve species collected near the Deliçay River (Karayakar et al., 2007) have also revealed high concentrations of heavy metals (e.g., Cd, Cr, Cu, Pb, and Zn) in their soft tissues. Soda-chromium chemicals industry in Kazanlı was held responsible for the high levels of metals in both soil and water (Koleli and Halisdemir, 2005) and highly criticized for stockpiling toxic chromium wastes (amounting 1.5×10^6 tons) on alluvial soils and releasing a variety of toxic chemicals into the nesting beach and the sea (Wolf, 2001; MEDASSET, 2001, 2009).

2.3. Geological and hydrogeological setting

The study area (TCP) is situated at the foothills of the central Taurus Mountains (i.e., Bolkar Mountains), which is represented by three distinct geologic units (Schmidt, 1961; Şenol et al., 1998). These are: (1) Carboniferous–Cretaceous basement rocks; (2) Tertiary sedimentary rocks; and (3) Quaternary–Recent deposits. Basement rocks include Permo-Carboniferous Karahamzauşağı formation and upper Cretaceous Mersin ophiolitic mélange. Karahamzauşağı formation is the oldest rock unit of the region, which consists of marble, dolomite,

and schist (Ünlügenç, 1986). Mersin ophiolitic mélange mainly outcrops within the drainage basin of the Deliçay River and contains substantial amounts of chromite mineralizations with Cr_2O_3 contents varying between 52% and 60% (Yaman, 1991). The basement rocks are unconformably overlain by a thick succession of Tertiary (Miocene–Pliocene) sedimentary rocks that outcrop mostly in the highlands at north. Tertiary units consist of a succession of marine, lacustrine, and fluvial deposits that display a transitional character both vertically and areally (Yetiş et al., 1995; Şenol et al., 1998). Tertiary sedimentary rocks are composed of lower-middle Miocene Karaisalı and Güvenç formations (limestone and clayey limestone, respectively) and middle-upper Miocene Kuzgun formation (sandstone, conglomerate, and limestone). This terrestrial and fluvio-deltaic deposition in the region was followed by the deposition of a mixed clastic-carbonate-evaporite succession in the Messinian (due to the desiccation of the Mediterranean Sea during the Messinian salinity crisis), which is represented by upper Miocene–Pliocene Handere formation (clay–siltstone, marl, limestone, sandstone, and gypsum) (Yetiş et al., 1995; Burton-Ferguson et al., 2005). In the study area, Tertiary sedimentary rocks are deeply buried under the unconsolidated fluvio-deltaic sediments of Quaternary–Recent in age (Yetiş and Demirkol, 1986). Fig. 3 presents the geological cross-sections through TCP based on data obtained from well logs (DSİ, 1978). Transects I–I′ and II–II′ traverse the plain in NW–SE direction and the transect III–III′ run nearly perpendicular to the former two in a SW–NE direction. In the area, Quaternary–Recent sediments show considerable variations in thicknesses (30 m in the north and >300 m in the south) and mostly consist of recent deposits of the Deliçay, Tarsus, and Seyhan rivers (Göney, 1976; DSİ, 1978). In most places, these deposits display a very heterogeneous character with laterally discontinuous layers that are composed of clay, silt, sand, and gravel, with the clay components dominating. Coastal part of the study area is mostly covered by well-sorted fairly loose recent eolian sand dunes that present an undulating topography in the area. For a detailed discussion on the general stratigraphy and geology of the TCP and the surrounding region, the reader is referred to a recent article by Gül (2007).

In the area, groundwater derived from the underlying Quaternary–Recent fluvio-deltaic coastal aquifer is heavily relied upon for agricultural, industrial and domestic water demands. From the lithologic well logs (see Figs. 2 and 3), it can be inferred that the aquifers in the coastal plain are mostly confined or semi-confined (i.e., under artesian pressures) in nature due to the presence of thick (20–100 m) clay–silt layers or lenses. Hydraulic head measurements conducted in the groundwater wells (in 2008) indicate that the confining layers are slightly permeable and allow the slow upward seepage of the groundwater. Even though it is a rare occurrence in the area today (due to extensive drainage efforts), earlier studies (e.g., DSİ, 1978) report the presence of free flowing artesian wells along the coastal zone. The hydraulic properties of the fluvio-deltaic deposits in the TCP are highly variable in space, which is typical of highly heterogeneous deltaic systems of the region (Gürbüz, 1999). In-situ Guelph permeameter tests ($n = 208$) conducted in the area (at a soil depth of ~35 cm) revealed that saturated hydraulic conductivities (K_{fs}) of the surficial sediments range between 2.94×10^{-6} and 9.37×10^{-2} cm s^{-1} (mean is 3.62×10^{-3} cm s^{-1} and variance = 1.01×10^{-4}). There is an apparent gradual increase in K_{fs} values of surficial sediments from north to south (i.e., hinterland to shore), which corresponds to a decrease in the percentage of clay- and silt-sized fractions (decreasing from a maximum of 74% in the north to 5% in the south) in deltaic sediments.

3. Materials and methods

3.1. Groundwater level measurements

A groundwater level survey was performed at the site during August 2008. Groundwater levels (depth to groundwater) in the

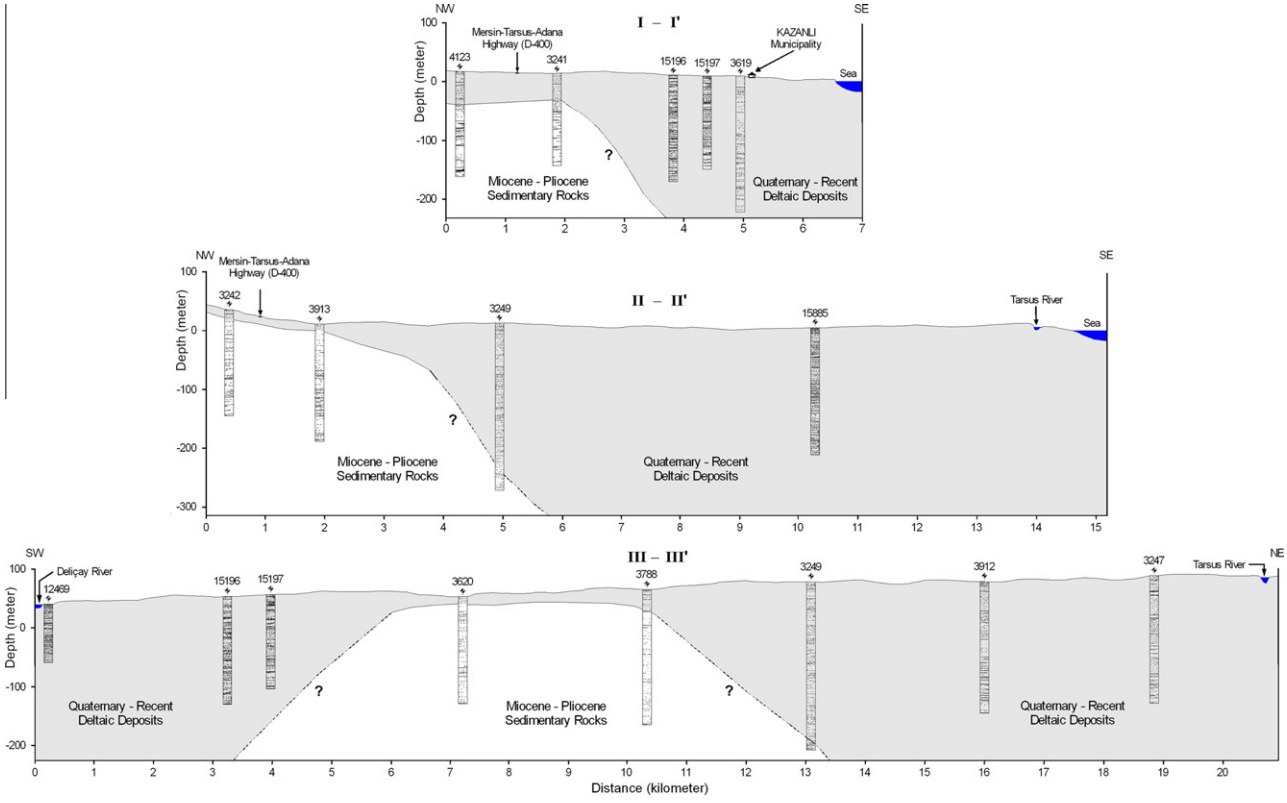

Fig. 3. Geological cross-sections through the Tarsus coastal plain (adapted from DSİ, 1978). The location of cross-sections I–III and lithologic well logs are presented in Fig. 2.

wells (n = 87) were determined manually using a water level meter (i.e., dip-meter) having a sensitivity of 1 mm. Groundwater elevations (with respect to MSL) were calculated in a GIS platform by subtracting depth to water measurements from the topographic elevations obtained from the digital elevation model (with a grid size of 2.5 m) of the site. Then, groundwater elevation values were contoured using the ordinary kriging (OK) spatial interpolation method available in the Geostatistical Analyst extension of the ArcGIS 9.3 software (ESRI, 2009). Additionally, for comparison purpose, historic groundwater levels were digitized from an earlier study (DSİ, 1978) conducted in the area.

3.2. Sample collection and treatment

A total of 193 wells were selected for the characterization of physico-chemical properties of the groundwaters. Additionally, 10 surface water samples were collected from various locations of the Deliçay and Tarsus rivers (DR1, TR1, TR2, and TR3), irrigation and drainage canals (IC1, DC1, DC2, and DC3), and the Mediterranean Sea (SW1 and SW2) (Fig. 2). All water samples were collected in a single sampling campaign during August 2008. All the wells chosen for groundwater sampling were commonly utilized for irrigation water supply and/or domestic purposes. Groundwater wells residing within the premises of the industrial facilities could not be sampled due to various reasons. Geographic coordinates of each sampling site were recorded with a handheld GPS unit (Magellan SporTrak) using UTM coordinate system and WGS84 datum. In order to ensure that the groundwater samples were representative of the in situ conditions, samples were collected after at least three well-bore volumes had been purged. Before sampling, the physico-chemical parameters of the waters were measured on-site using temperature-compensated WTW Multi 340i/SET multi-parameter instrument (Wissenschaftlich-Technische Werkstätten, Germany), equipped with electrical conductivity (EC), dissolved oxygen (DO), and pH probes. The probes were calibrated using appropriate standard solutions or procedures before sampling of the waters. Two aliquots of sample were collected into 250 mL high-density polyethylene bottles from each sampling location; one for cation and the other for anion analysis. Aliquots taken for cation analysis were acidified at the field to pH < 2 with analytic grade nitric acid. The samples were stored in an esky containing ice packs to prevent possible evaporation effects. Then, they were transported to the laboratory and refrigerated at 4 °C until analysis.

3.3. Analytical procedures

All analyses were carried out at the Mersin University Geological Engineering Department, Mersin, Turkey. The concentrations of chloride (Cl^-), sulfate (SO_4^{2-}), fluoride (F^-), nitrate (NO_3^-), and nitrite (NO_2^-) were determined using Hach Lange DR 2800 spectrophotometer (Hach Lange GmbH, Düsseldorf, Germany). Bicarbonate (HCO_3^-) was determined in the laboratory by volumetric titration according to EPA 310.1. Analyses for total concentrations of five major elements (Ca, Mg, Na, K, and Si) and nine trace elements (B, Ba, Br, Cr, Fe, Mn, Ni, Sr, and Zn) were carried out (in separate batches) with inductively coupled plasma-mass spectrometry (ICP-MS). Concentrations of elements in the samples were determined in triplicate by Agilent 7500ce ICP-MS (Agilent Technologies, Tokyo, Japan) equipped with Octopole Reaction System. The external standard calibration method was applied to all determinations, using ^{6}Li, ^{45}Sc, ^{72}Ge, ^{89}Y, ^{115}In, and ^{209}Bi internal standard mix. Five-point calibration curves were constructed by analyzing

Table 2
Descriptive statistics of the 24 physicochemical parameters of the groundwater (n = 193) and surface water (n = 10) samples collected from the Tarsus coastal plain (TCP).

Parameters	Unit	Groundwater (n = 193)				Surface water (n = 10)									
		August 2008 samples				Tarsus river			Deliçay river	Drainage canals			Irrigation canal	Mediterranean seawater	
		Min.	Max.	Median	MAD	TR1	TR2	TR3	DR1	DC1	DC2	DC3	IC1	SW1	SW2
EC[a]	µS cm^{-1}	431.0	2991.0	906	143.0	602.0	577.0	705.0	657.5	2270.0	2500.0	1229.0	329.0	57,100	58,400
TDS[b]	mg L^{-1}	336.1	2307.4	704.9	121.3	442.5	417.4	491.2	407.4	1441.4	1556.4	895.4	266.8	37,246	37,794
DO[c]	mg L^{-1}	0.4	5.2	1.7	0.66	4.3	3.9	2.2	4.0	2.6	4.0	6.7	4.6	4.4	4.6
pH	Standard	7.0	8.7	7.5	0.25	7.9	7.8	7.7	8.3	7.5	7.7	8.3	7.8	7.8	8.2
Ca^{2+}	mg L^{-1}	8.4	223.3	79.5	24.4	59.4	56.2	62.3	54.2	89.2	80.9	67.0	51.6	785	808
Mg^{2+}	mg L^{-1}	4.6	176.1	41.8	13.9	22.7	17.9	23.2	27.3	48.9	58.7	39.4	9.4	1488	1576
Na^{+}	mg L^{-1}	7.8	410.6	53.0	28.6	44.0	39.1	69.9	32.5	360.9	389.2	157.5	11.8	10,200	10,190
K^{+}	mg L^{-1}	0.7	99.1	2.2	0.83	2.5	3.0	3.6	2.1	18.2	13.9	4.9	1.2	449	529
Si	mg L^{-1}	3.9	27.9	15.2	6.3	4.5	4.6	4.7	1.9	6.7	8.9	6.5	7.2	3.3	4.1
Cl^-	mg L^{-1}	6.1	433.0	67.8	31.8	30.2	51.0	26.8	28.3	560.0	444.8	165.3	11.1	21,150	21,100
SO_4^{2-}	mg L^{-1}	1.0	741.0	73.6	29.6	57.0	53.0	61.0	32.5	130.0	118.0	151.8	13.0	2900	3312
HCO_3^-	mg L^{-1}	140.7	667.8	297.2	56.5	184.3	161.6	227.0	269.6	213.7	404.1	224.2	137.8	89.7	86.4
F^-	mg L^{-1}	0.1	1.3	0.34	0.13	0.2	0.2	0.2	0.7	1.6	0.3	0.4	0.2	1.9	2.9
NO_3^-	mg L^{-1}	0.4	201.1	11.1	9.7	5.3	7.5	6.2	4.9	3.5	3.5	0.9	2.7	5.8	9.3
NO_2^-	mg L^{-1}	0.0	2.4	0.02	0.01	0.2	0.3	0.3	0.6	0.3	0.1	0.0	0.1	0.4	0.1
B	µg L^{-1}	42.9	1920.0	150.0	83.3	68.8	94.4	106.3	–	288.2	987.7	256.4	287.8	11,780	3387
Ba	µg L^{-1}	10.2	249.0	58.2	15.6	49.0	51.4	43.6	30.6	69.9	39.1	26.8	22.2	97.5	145.1
Br	µg L^{-1}	21.9	1532.0	190.3	82.8	80.1	78.9	140.0	–	1945.0	2576.0	481.6	41.2	73,960	88,330
Cr	µg L^{-1}	0.1	62.8	3.6	3.1	1.7	1.3	1.3	2.3	1.2	0.8	1.2	0.5	102.6	520.9
Fe	µg L^{-1}	0.1	2052.0	63.9	52.1	476.8	593.1	277.3	183.4	307.2	168.4	252.1	78.9	1058	3710
Mn	µg L^{-1}	0.1	259.2	2.1	2.1	43.1	78.9	24.2	21.4	62.6	23.9	24.9	7.7	915.3	257.5
Ni	µg L^{-1}	1.5	43.7	3.9	1.0	7.0	7.0	6.6	9.4	5.9	5.2	6.7	4.7	705.7	449.4
Sr	µg L^{-1}	116.0	6001.0	839.1	304.9	433.8	404.4	419.2	392.4	952.7	688.5	564.7	244.3	10,200	9762
Zn	µg L^{-1}	2.5	4593.0	79.8	70.2	10.6	11.7	10.3	11.8	10.2	3.9	5.8	61.4	355.5	4703

Min.: minimum, Max.: maximum, MAD: = median absolute deviation (see Reimann et al., 2005).
For the locations of surface water samples (TR1, TR2, TR3, DR1, DC1, DC2, DC3, IC1, SW1, and SW2) please see Fig. 2.
[a] Electrical conductivity.
[b] Total dissolved solids (calculated as sum of all ions).
[c] Dissolved oxygen.

NIST single-element reference standards prepared by serial dilution of stock solutions. The ultrapure water (ELGA Purelab UHQ, UK) used throughout the period of experimentation had a resistivity of 18 MΩ cm at room temperature. The accuracy and precision of the analytical technique was evaluated by analyzing a certified standard reference material, Certified Waste Water Trace Metals Solution (B) (High-Purity Standards, Charleston, SC, USA). The relative error is less than ±5% for all analyzed elements. Additionally, as an independent check on the accuracy of the analytical results, the percent charge balance errors (%CBE) were calculated for each water sample as suggested by Freeze and Cherry (1979). Calculated charge balance errors are less than ±5%, with a mean value of 0.2%. The descriptive statistics of the groundwater and surface water chemistry data are summarized in Table 2. The geochemical code PHREEQC (ver. 2) (Parkhurst and Appelo, 1999) was used to evaluate aqueous speciation and calculate the saturation indices for phases (i.e., minerals) employing the default database (phreeqc.dat).

3.4. The fuzzy c-means (FCM) clustering

Clustering techniques fall into two main categories: they are considered to be "hard or crisp" if an object (i.e., water sample) belongs exclusively to a single class or "soft or fuzzy" if an object belongs to all classes in varying degrees of membership (Güler and Thyne, 2004). All fuzzy clustering algorithms rely on elements of the fuzzy-set theory (Zadeh, 1965) and many of them are based on the fuzzy *c*-means (FCM) clustering algorithm, originally proposed by Dunn (1974) and extended by Bezdek (1981). Fuzzy logic is basically a multi-valued logic that allows intermediate values to be defined between conventional binary evaluations like yes/no, true/false, white/black, 1/0, etc. (Fang and Chen, 1990). The heart of the fuzzy-set theory is the membership function, which represents numerically the degree to which an object belongs to a set. As a multivariate data analysis technique, FCM clustering (Bezdek, 1981) partitions a data set, $\boldsymbol{X} = \{x_1, \ldots, x_n\} \subset \mathcal{R}^p$, into $c \in \{2, \ldots, n-1\}$ overlapping or fuzzy classes, which are identified by their class centers (or prototypes), v_i ($i = 1, \ldots, c$). The partitioning of data into fuzzy classes is achieved by minimizing the objective function:

$$J_{FCM}(\boldsymbol{M}, \boldsymbol{C}) = \sum_{i=1}^{c} \sum_{k=1}^{n} u_{ik}^{m} \|X_k - v_i\|^2 \quad (1)$$

using an iterative procedure (see Güler and Thyne, 2004). In Eq. (1), $\boldsymbol{M}$ is the membership matrix, $\boldsymbol{C}$ is the class centers matrix, c is the number of classes (groups), n is the number of data points, and u_{ik} is the degree of membership of sample k in class i. If the Euclidean distance between datum x_k and class center v_i is high, J_{FCM} is minimized. If the distance is small, the membership value approaches unity (Höppner, 2002). The parameter $m \in (1, \infty)$ is a weighting exponent that controls the degree of the fuzziness of the resulting classification, which is the degree of overlap between classes. When $m = 1$, the solution is a hard partition, that is, the result obtained is either 0 (non-member) or 1 (member). As m approaches infinity (∞) the solution approaches its highest degree of fuzziness (Bezdek, 1981). Bezdek et al. (1984) and Güler and Thyne (2004) provides a more detailed discussion on the FCM clustering algorithm and examples can be found in Bezdek et al. (1999).

Soft clustering techniques are useful, since they allow meaningful generalizations to be made about large quantities of data by extracting basic patterns. In FCM, the number of classes (c) and the value of fuzzification parameter (m) need to be determined at the start of the analysis. There are several functions, so-called "validity functions", that can be used to determine the optimum values of c and m. In this study, validity functions introduced by Bezdek (1981), Roubens (1982), and Xie and Beni (1991) have been used. In FCM results, the membership of objects is graded (partitioned) between classes with membership values (u) ranging between 0 and 1, thus eliminating the sharp boundary dividing members of the set from non-members. This type of partitioning may provide more information about the data set at hand and enables us to consider partial memberships that can have some sort of meaning (e.g., geological, hydrological, hydrochemical, spatial, etc.).

3.5. Principal components analysis (PCA)

As a multivariate statistical data analysis technique, PCA can provide a powerful tool for analyzing high dimensional hydrochemical data sets. This multi-step approach has been applied successfully to extract related variables and infer the underlying natural and/or anthropogenic processes that control the chemistry of groundwaters (Helena et al., 2000; Güler et al., 2002; Thyne et al., 2004). PCA technique reduces a large number of variables (i.e., measured physico-chemical parameters of water samples) to a small number of principal components (i.e., PCs) by linearly combining measurements made on the original variables (Davis, 1986). In PCA analysis; the axes (PCs) may represent the dominant underlying natural or anthropogenic processes and by definition they are uncorrelated with each other. Varimax rotation is generally applied to the PCs in order to reduce the contribution of variables with minor significance (Closs and Nichol, 1975). Because of the ability of PCA to achieve a variance-maximizing rotation, all variability in the variables can be accounted for. There are several criteria for determining the number of PCs to be extracted including (but not limited to): "Kaiser criterion", "Cattell scree plot", and "Explained variance criterion". The "Kaiser criterion" (Kaiser, 1960) takes into account only PCs with eigenvalues greater than 1.0, where unless a PC extracts at least as much information as the equivalent of one original variable, it is discarded (Hill and Lewicki, 2007). In "Cattell scree plot" method (Cattell, 1966), the number of components and their corresponding eigenvalues are plotted on the *x*- and *y*-axes, respectively. In this diagram, change in the gradient of the line (i.e., elbow) marks the number of components, where components beyond the break point are thrown away (Hill and Lewicki, 2007). "Explained variance criterion" is simply used to keep enough components (PCs) to account for 90–95% or sometimes as low as 50–55% of the variation. All these different criteria should be applied prudently to keep the number of components in a manageable size (i.e., preferably less than six PCs) for visualization purposes.

In general, the purpose of the PCA in hydrogeologic studies is (1) to find variables (physical or chemical) that are good descriptors of the groundwater system and important in the processes occurring in the area under investigation and (2) to select components in an objective way without losing essential information. Therefore, the primary purpose of the PCA is data reduction and summarization. Researchers routinely performing PCA know that finding an optimal solution is a tedious multi-step process which requires elimination of some initial variables, hopefully explaining various processes or factors in the area of interest – without *a priori* knowledge about their nature and numbers. Some researchers call this cleaning process as "noise reduction", where only the most important variables are retained at the end and the least important ones (creating the noise) are eliminated. During "noise reduction" process in PCA, the following steps are usually taken into consideration, although cutoff values chosen vary in the literature:

- Variables with loadings below a pre-determined threshold value (i.e., ±0.7) are generally considered insignificant and can be eliminated from the PCA matrix.
- Communalities for each variable should be close to 1. In other words, variables with low communality values (i.e., <0.7) can also be eliminated from the PCA matrix.

- Similarly, PCs with eigenvalues smaller than 1 are considered insignificant (Kaiser Criterion) and therefore can be eliminated from the final model. Cattell scree plot also provides a good estimate about the number of PCs that should be retained.

For the PCA in our study, we started with 24 physico-chemical variables available in our dataset. Our final PCA model only includes 16 variables (Ca, Mg, Na, Cl, SO_4, F, HCO_3, NO_3, B, Br, Cr, Fe, Mn, Ni, Sr, and Zn) where they were combined to produce four significant PCs explaining 73.34% of the variance of the original dataset. We have also experimented with different number of factors (as much as 10) within the limits or constraints imposed by the PCA method (Hill and Lewicki, 2007). The reader is referred to the work of Davis (1986) for an in-depth account of the theory. The paper by Costello and Osborne (2005) also provides an excellent review of the method and provide practical information on "best practices" in the use of PCA.

4. Results and discussion

4.1. Groundwater levels and flow directions

Groundwater level surveys provide valuable information on the groundwater gradients and flow directions. This type of survey can also aid qualitative estimates of the flow paths and facilitate a better definition of the extent of the hydrologic system. In Fig. 2, comparison of pre 1978 (dashed red line) and 2008 (solid blue line) groundwater levels clearly shows the combined effects of the heavy groundwater pumping and extensive drainage efforts on the hydrology of the area. In the past three decades, groundwater levels and flow directions in the area have been drastically modified by human activities (Fig. 2), which in turn, not only resulted in local declines in groundwater levels (2–5 m) but also deteriorated the water quality to unacceptable levels in the coastal part. Increases in groundwater EC values and concentrations of Na^+, Cl^-, B, and Br (data not shown) confirm the presence of active seawater intrusion at the coastal part, especially in the area between Kazanlı and Kulak settlements (Fig. 2). In the southern part of the transect stretching from Kazanlı to Bahşiş settlements (Fig. 2) a superficial aquifer has also been established just below the ground surface (depth to water < 1 m) and large areas become waterlogged during the wet winters. In this study, 491 individual water bodies were digitized from the Quickbird satellite images (see Fig. 1). These small artificial lakes, covering a total area of 0.88 km^2, were mostly originated by extraction of sand and gravel from the coastal zone. The extracted material is mostly used for leveling the uneven ground surface (due to sand dune topography) around the greenhouses. In TCP, the general direction of groundwater flow in the aquifer system is from NW to SE (Fig. 2), with an average hydraulic gradient of ~2‰.

In TCP, recharge to the aquifer takes place through several mechanisms including direct precipitation, subsurface inflows from the northern side of the plain (from the recharge area), seepages from the canal network and irrigation runoff, inflows from the Deliçay and Tarsus rivers, and the seawater intrusion near the coastal settlements such as Kazanlı and Kulak (Fig. 2). Whereas, groundwater discharge in the area occurs by a number of ways such as; groundwater abstraction via wells, evapotranspiration, and discharge from springs, seeps and open drainage canals. Beside groundwater wells, irrigation water for agriculture in the area is supplied from an open canal network. The return flow from surface runoff and the surplus of irrigation water is collected by a drainage canal network and then disposed of into the Mediterranean Sea and Tarsus River (see Fig. 2 and Table 2).

4.2. Fuzzy classification and spatial distribution of the FCM classes

Fuzzy (soft) classification of the hydrochemical data set into overlapping and continuous classes was performed using the FCM clustering algorithm (Bezdek et al., 1984). Of the 24 physico-chemical variables available in the data set (Table 2), 15 selected variables (Ca^{2+}, Mg^{2+}, Na^+, K^+, Si, Cl^-, SO_4^{2-}, F^-, NO_3^-, NO_2^-, B, Ba, Br, Sr, and Zn) were utilized in the FCM classification. These variables were also considered as being of primary significance in terms of delineating hydrochemical facies distribution in the TCP area. Kolmogorov–Smirnov (K–S) normality test results have shown that all variables are log-normally distributed ($p < 0.05$). Therefore, as suggested by Güler and Thyne (2004), all variables were log-transformed (base 10) and then standardized to their standard scores (z-scores) before applying FCM method. In FCM clustering, not only the number of classes (c) is pre-selected but the choice of metric distance, stopping criterion (ε), and fuzzification parameter (m) value has to be defined *a priori*. In this study, Euclidean distance was chosen as the distance measure and a value of 1×10^{-3} was used for ε. For the selection of the optimal c and m values, the cluster validation functions introduced by Roubens (1982) (e.g., fuzziness performance index; FPI and normalized classification entropy; NCE) and by Xie and Beni (1991) (e.g., compactness & separation measure; S) have been used. Additionally, the derivative of J_{FCM} with respect to m, $-[(\delta J_{FCM}/\delta m)c^{0.5}]$ was also used to assist in determining the optimal values of c and m (see Bezdek, 1981 and McBratney and Moore, 1985). To determine the optimum classification parameters, the TCP data set was partitioned into a range of c (between 2 and 10) and using a series of m values (i.e., 1.05, 1.10,...,2.00) at an increment of 0.05. Using this procedure, the data set was clustered with different combinations of c and m values. From the trial runs it appeared that $m = 1.35$ resulted in membership values that were neither too fuzzy nor too hard for spatial mapping purposes. Plots of FPI, NCE, and S versus the c values were presented in Fig. 4. As it is seen in Fig. 4a and b, both FPI and NCE values are minimal at $c = 4$ for $m = 1.35$. This means that the optimal number of classes in the data set is 4. Plots of S versus the c values in Fig. 4c and $-[(\delta J_{FCM}/\delta m)c^{0.5}]$ versus the m values in Fig. 4d also confirms this result. Therefore, for this study the optimum number of classes and fuzzification parameter value were chosen to be 4 and 1.35, respectively. This set of parameter values has also resulted in a hydrogeologically meaningful class distribution and geographically coherent maps in the study area (see Fig. 5).

Both the physical and chemical meaning of the FCM-determined classes can be interpreted in view of the class centers (i.e., prototypes). Tables 3 and 4 present the representative parameter values (for physico-chemical parameters and trace elements, respectively) of the four class centers (i.e., C1, C2, C3, and C4) derived by FCM objective function. In Tables 3 and 4 representative parameter values for the membership threshold values (u_T) of 0.50 and 0.75 showed a little variation. Hence, in this study, the membership threshold value was fixed at 0.50 and used for calculation of class centers and for the spatial mapping purposes. More than 57.5% of the water samples in the area are classified as Class 1, which is distinguished from the other three classes by its lower EC, Na^+, K^+, Cl^-, SO_4^{2-}, F^-, B, Ba, Br, and Mn values and higher DO, Cr, and Zn values (Tables 3 and 4). Class 2 is the second most prominent water type (27.5% of the samples) in the area and it is distinguished from other classes by its lowest Ca^{2+}, Mg^{2+}, HCO_3^-, NO_3^-, and NO_2^- values and intermediate values for the rest of the parameters. Class 3 constitutes nearly 8.3% of the water samples and is characterized by high values of pH, Cl^-, Ba, Fe, and Mn and with a low value of DO. Class 4 has only five members and is chemically distinct from all the other classes. Members of this class are characterized by high values of EC, Ca^{2+}, Mg^{2+}, Na^+, K^+, Si, SO_4^{2-}, HCO_3^-,

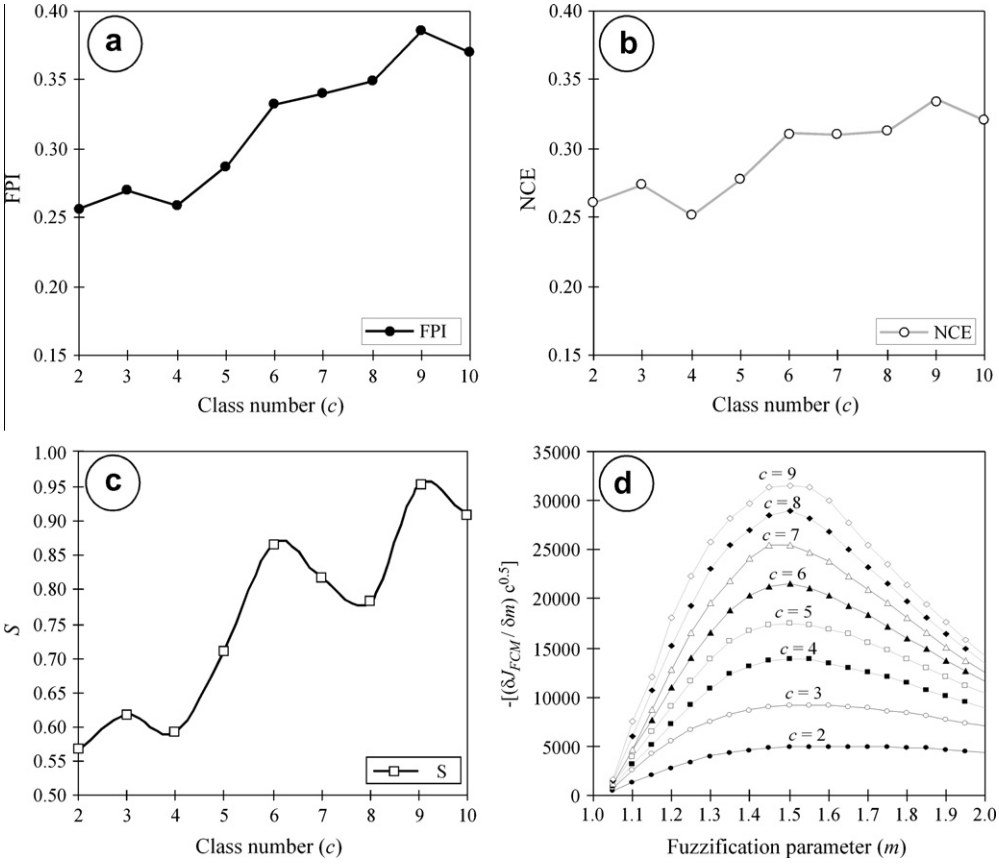

Fig. 4. Fuzzy *c*-means validity functions: (a) fuzziness performance index (FPI), (b) normalized classification entropy (NCE), and (c) compactness and separation measure (*S*) values against the number of classes for fuzzification parameter (m) = 1.35, and (d) $-[(\delta J_{FCM}/\delta m)c^{0.5}]$ against fuzzification parameter (m) = 1.05–2.00 for c = 2–9.

F^-, NO_3^-, NO_2^-, B, Br, Ni, and Sr. Members of Class 4 also display the lowest values for pH and Fe (Tables 3 and 4). Highly variable nature of the data indicates the complex nature of the underlying hydrological and/or hydrochemical phenomena at the site.

Fig. 5 presents the results from the FCM clustering on map view. For the preparation of this map and to define the fuzzy hydrochemical class distribution in the study area, the membership values (u) of groundwater samples (n = 193) were separately interpolated for each water class (i.e., C1, C2, C3, and C4) on a regular grid by the OK method. All geostatistical calculations (i.e., variogram modeling, cross validation, and spatial analyses) were carried out using the Geostatistical Analyst extension available in the ArcGIS 9.3 software (ESRI, 2009). From the geostatistical analyses, four different maps were obtained, each showing the membership value distribution of a particular class over the entire study area. Then, all four maps were overlaid using the GIS software to produce a composite map showing the distribution of fuzzy memberships of groundwater samples in all classes. For the visualization purposes and to achieve a better class separation, each class was color-coded and only membership values above 0.5 were plotted on the map. In Fig. 5, cluster memberships (u) range between 0.5 and 1.0, where lighter colors indicate a weak membership and darker colors indicate a strong membership to a particular water class. This mapping method also produces white-colored areas (Fig. 5) that indicate the transitional zones between classes (i.e., class boundaries), where membership of groundwater samples is divided between more than two classes (u < 0.5). Therefore, these samples do not belong to any particular class and they generally present unique water chemistries that result from various processes. This type of information cannot be obtained from hard partitioning techniques (e.g., hierarchical cluster analysis). As we can see in Fig. 5, the membership values for each class show distinctive spatial patterns and the FCM-determined four classes are well-separated in a geographical sense. This means that the spatial distribution of the FCM classes can be used to discuss the main features (both hydrologic and hydrochemical) of the TCP. This is a valid assumption since previous studies (e.g., Güler and Thyne, 2004) have shown that the samples that belong to same class generally have similar chemical properties due to similar underlying processes and/or groundwater flow paths. It should also be emphasized that the FCM clustering initially does not infer anything about the spatial distribution or contiguity of these classes (Lucieer and Lucieer, 2009). However, in order for the FCM-defined classes to be useful, their distribution should create a representation of the hydrologic system and mimic the hydrochemical evolution along the groundwater flow paths (Thyne et al., 2004). The observed changes in water chemistries (i.e., increase and decrease in elemental concentrations) along such a system is mainly related to natural water–rock interactions, however, in places where anthropogenic activities are intense, additional changes to groundwater chemistries should also be expected due to mixing with infiltrating surface waters and waste discharges. In this respect, interpretations made in this section are mainly based on the maps showing groundwater levels and flow directions (Fig. 2) and the FCM class distribution in the TCP area (Fig. 5). Hydrochemical significance of the FCM-defined classes will be discussed further in the following sections.

As it was mentioned previously, majority of the groundwater samples in the area were classified as Class 1 (n = 111). Strong members (u > 0.75) of the Class 1 are generally found in the western (near the Deliçay River) and eastern (near the city of Tarsus and the Tarsus

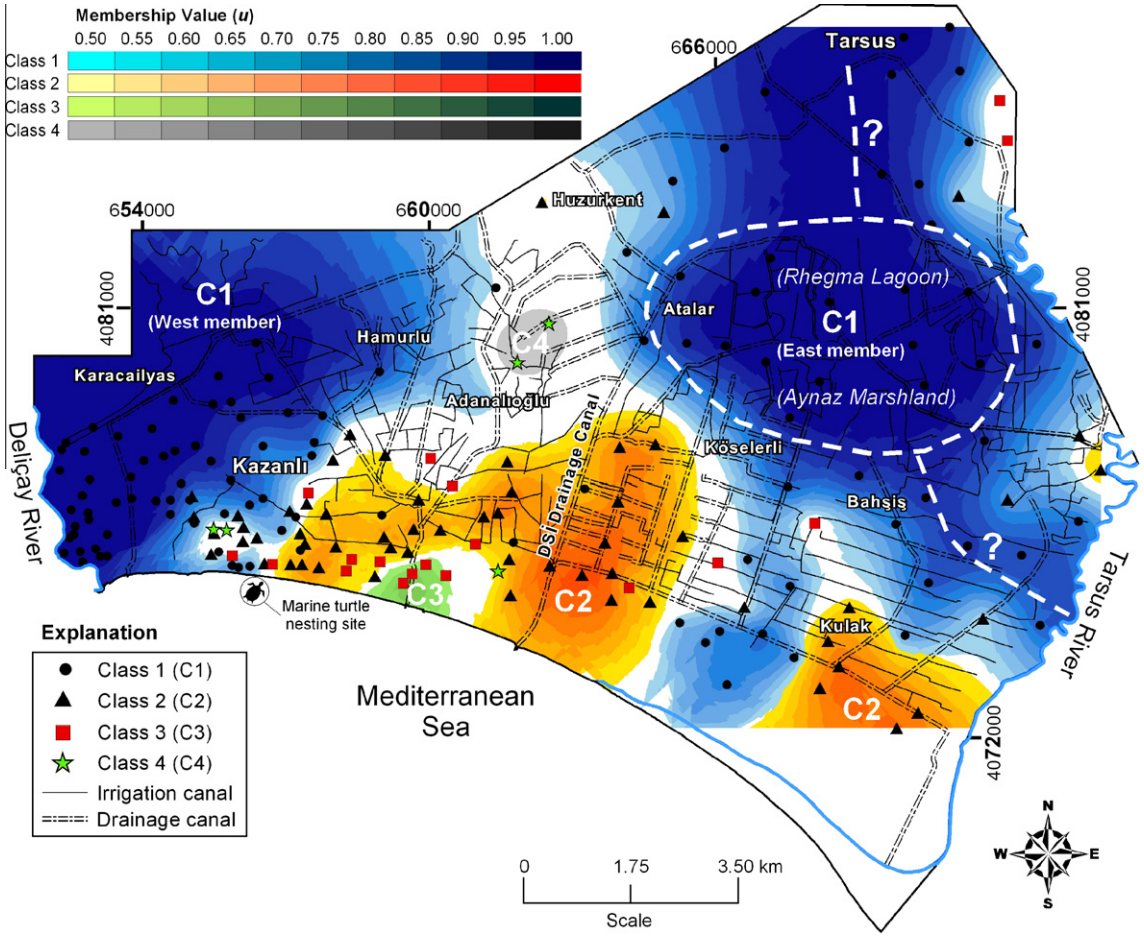

Fig. 5. Map showing the spatial distribution of memberships of the groundwater samples over four fuzzy classes determined by FCM objective function (for $m = 1.35$ and $u \geqslant 0.5$). Dashed white lines represent the approximate extent of the ancient Rhegma Lagoon (later Aynaz Marshland) and pre-diversion location of the Tarsus River before the 6th century (adapted from Rother, 1971).

Table 3
Representative values of the physicochemical parameters for four classes derived by FCM objective function. Class means were calculated using samples with membership values above 0.50 and 0.75.

FCM class	u_T[a]	n[b]	Physicochemical parameters													
			EC[c]	DO[d]	pH	Ca^{2+}	Mg^{2+}	Na^{+}	K^{+}	Si	Cl^{-}	SO_4^{2-}	HCO_3^{-}	F^{-}	NO_3^{-}	NO_2^{-}
C1	⩾0.50	111	816.1	2.35	7.46	86.4	45.6	36.0	3.2	14.7	47.9	67.4	316.5	0.30	20.4	0.096
	⩾0.75	106	816.2	2.39	7.45	85.4	46.3	34.6	3.2	14.8	46.2	66.7	316.7	0.29	21.1	0.100
C2	⩾0.50	53	966.0	1.62	7.76	62.4	39.5	107.5	4.8	14.6	120.7	91.1	260.8	0.42	8.4	0.046
	⩾0.75	41	945.3	1.58	7.79	60.2	36.6	109.4	3.8	14.1	129.3	86.3	244.9	0.41	5.4	0.030
C3	⩾0.50	16	1552.8	1.37	7.82	84.1	55.3	199.4	8.8	15.5	273.1	165.8	293.2	0.51	9.2	0.172
	⩾0.75	14	1589.9	1.44	7.78	89.9	59.0	193.7	9.6	15.4	283.5	176.1	291.3	0.48	10.4	0.194
C4	⩾0.50	5	2300.4	1.43	7.36	176.8	109.0	199.5	31.2	18.0	154.2	612.2	429.3	0.76	51.5	0.525
	⩾0.75	4	2488.3	1.60	7.38	191.6	105.1	235.0	33.5	17.2	177.0	659.3	436.6	0.85	59.0	0.626

All concentrations (except as noted) are in mg L^{-1}. pH is in standard units.
[a] Membership value (u) threshold used for calculation of FCM class means.
[b] Number of samples within respective FCM classes for indicated membership threshold values.
[c] Electrical conductivity (μS cm^{-1}).
[d] Dissolved oxygen (mg L^{-1}).

River) parts of the TCP (Fig. 5). Class 1 is divided into two components along a line stretching from Huzurkent to Adanalıoğlu settlements (Fig. 5). One of the reasons for this separation is probably the presence of a cone of depression between Huzurkent and Tarsus (Fig. 2), which has greatly modified the groundwater flow directions in the area. The other reason can be explained with the help of the geological cross-sections through the TCP (Fig. 3). In this part of the plain, a buried, S dipping promontory composed of Miocene–Pliocene formations (clay–siltstone–marl–limestone alternations containing gypsum) extends through 1/3 of the basin in N–S direction (cross section II–II′ in Fig. 3). This promontory divides the TCP into two sub-basins (cross section III–III′ in Fig. 3) and overlain by a thin veneer (30–40 m) of Quaternary–Recent fluvio-deltaic sediments (around Huzurkent). This shallow aquifer is represented by Class 4 waters and geographically located in between west and east members of the Class 1 (Fig. 5). Chemical quality of the Class 4

Table 4
Representative values of the trace elements for four classes derived by FCM objective function. Class means were calculated using samples with membership values above 0.50 and 0.75.

FCM class	u_T[a]	n[b]	Trace elements								
			B	Ba	Br	Cr	Fe	Mn	Ni	Sr	Zn
C1	⩾0.50	111	150.9	60.3	161.4	7.86	141.3	11.4	5.20	964.9	440.7
	⩾0.75	106	152.4	59.9	158.9	7.51	138.3	11.0	5.26	895.0	440.1
C2	⩾0.50	53	249.9	60.9	263.4	4.67	189.8	16.0	3.43	924.1	271.3
	⩾0.75	41	248.1	57.9	237.3	4.05	185.9	15.2	3.36	922.2	168.0
C3	⩾0.50	16	342.6	68.0	636.8	1.80	252.3	43.7	5.67	1161.6	148.5
	⩾0.75	14	339.2	71.2	669.9	1.95	278.5	49.2	6.21	1213.2	165.2
C4	⩾0.50	5	929.7	62.6	677.2	2.89	100.9	38.0	9.46	3170.8	346.6
	⩾0.75	4	1102.0	54.6	760.3	1.73	100.3	47.3	10.56	3663.0	410.5

All concentrations are in $\mu g\,L^{-1}$.
[a] Membership value (u) threshold used for calculation of FCM class means.
[b] Number of samples within respective FCM classes for indicated membership threshold values.

waters is not suitable for most consumptive purposes due to high concentrations of several chemical constituents (e.g., Ca^{2+}, Mg^{2+}, Na^{+}, K^{+}, Cl^{-}, and SO_4^{2-}) (Table 3). High concentrations of these chemical constituents in Class 4 waters can be explained by dissolution of evaporitic series in Miocene–Pliocene formations. Groundwater wells drilled in Miocene–Pliocene formations have also low yields (indicated by drillers' notes on the well logs) due to presence of thick clay–siltstone–marl alternations. Groundwater flow directions in Fig. 2 suggest that west and east members of the Class 1 are probably a mixture of recharge waters entering the basin from the northern side and inflows from the Deliçay and Tarsus rivers in their lower reaches, respectively. Similarities in the physico-chemical properties of Class 1 waters (Tables 3 and 4) and the river samples (TR1-3 and DR1) (Table 2) also confirm this hypothesis. A peculiar characteristic of the east member of Class 1 is that strong members ($u > 0.75$) of this class mostly occur along the pre-diversion Tarsus River channel and in the area once occupied by the ancient Rhegma lagoon (or as it was later called Aynaz marshland) (Fig. 5). Even though these ancient geographic features are deeply buried (by mostly wind-blown sediments) and therefore not visible on the surface today, hydrochemical evidence suggest that groundwater flow possibly occurs preferentially along the pathways inherited from the pre-existing subsurface paleo-river channels and the deposits infilling the ancient lagoon area (see Figs. 2 and 5).

In the area, excessive groundwater pumping and extensive drainage efforts have collectively resulted in the formation of local cone of depressions near the coastal settlements such as Kazanlı, Adanalıoğlu, Kulak, Bahşiş, and Köselerli (Fig. 2). Consequently, this has resulted in salinization (i.e., seawater intrusion) of the coastal zone along a line extending eastward from Kazanlı to Kulak and northward to Adanalıoğlu settlements (Figs. 2 and 5). In TCP, these saline waters are represented by Class 2 and Class 3 in the area (Fig. 5) and their representative parameter values are given in Tables 3 and 4 (discussed in detail in Section 4.3.2).

4.3. Factors affecting the groundwater chemistry in TCP

In a broad sense, the chemical composition of groundwater reflects the chemical composition of the geologic units found in the drainage basin and provides valuable information on the presence of contaminants from anthropogenic sources and/or contributions from external sources (e.g., inflows from the rivers, canals, and the sea). In anthropogenically disturbed environments, PCA technique can highlight those groups of samples or outliers that are controlled by such factors from the more pervasive natural background (Thyne et al., 2004). In this study, PCA was used to identify the variables most important to separating the classes, in effect extracting the components that control the chemical variability in groundwater samples. In this study, log-transformed and standardized data matrix was used in the PCA as described by Güler et al. (2002) to give each variable equal weight in the multivariate statistical analysis. Statistical software R (ver. 2.5.1) (R Development Core Team, 2007) was used to perform the PCA. Rotation of PCs was carried out using the varimax method, where both Kaiser criterion and Cattell scree plot were used to determine the number of components.

The end result of a PCA is two matrices of numbers such as PC loadings (Table 5) and varimax component scores (not shown in a table form here, but presented as Fig. 6). In this study, by applying the PCA technique, 16 variables (Ca^{2+}, Mg^{2+}, Na^{+}, Cl^{-}, SO_4^{2-}, F^{-}, HCO_3^{-}, NO_3^{-}, B, Br, Cr, Fe, Mn, Ni, Sr, and Zn) were combined to produce four significant PCs explaining 73.34% of the variance of the original data set (Table 5). However, to give physical significance to the PCs requires a good geochemical understanding of what the original variables mean. As suggested by Dalton and Upchurch (1978) component scores can be related to intensity of the chemical process described by each PC, where extreme negative scores (<−1.0) reflect areas essentially unaffected by the process and positive scores (>+1.0) reflect areas most affected. Near-zero scores approximate areas affected to an average degree by the chemical process of that particular PC. Therefore, varimax component scores of groundwater samples ($n = 193$) were separately interpolated for each PC (i.e., PC1, PC2, PC3, and PC4) on a regular grid by the OK method using ArcGIS 9.3 software (ESRI, 2009). Fig. 6 shows the spatial distribution of the component scores for each of the four PCs, in effect visualizing the intensity of the dominant underlying chemical process occurring at the site. To aid in the interpretation process, saturation indices (SI) of minerals (calcite, dolomite, gypsum, and halite) were also calculated using PHREEQC (ver. 2) computer program (Parkhurst and Appelo, 1999) and the results are presented in a map form in Fig. 7.

4.3.1. PC1 – Water–rock interaction and nitrate contamination

Most of the variance in the original data set is contained in the PC1 (28.8%), which is associated with the variables Ca^{2+}, Mg^{2+}, SO_4^{2-}, HCO_3^{-}, Sr, Ni, and NO_3^{-} (with loadings between 0.602 and 0.926) (Table 5). PC1 contains both classical hydrochemical variables, such as; Ca^{2+}, Mg^{2+}, SO_4^{2-}, HCO_3^{-}, Sr, and Ni originating from the natural weathering processes of sedimentary/evaporitic/ophiolitic rocks (e.g., limestone/dolomite, gypsum, and ophiolite) found in the recharge areas and nitrate (NO_3^{-}) that indicates the occurrence of a non-point pollution, possibly from agricultural sources such as fertilizer application. In most other studies of this type, water–rock interaction and nitrate contamination are diametrically opposed, i.e., most nitrate contamination is evident in groundwater with the least evidence of water–rock interaction and vice versa (Helena et al., 2000; Adams et al., 2001; Mahlknecht

Table 5
Component loadings (varimax rotated) for groundwater samples of the Tarsus coastal plain (n = 193).

Variables	Principal components			
	PC1	PC2	PC3	PC4
Ca^{2+}	**0.926**	0.004	0.114	0.011
Mg^{2+}	**0.783**	0.144	0.184	0.165
Na^{+}	−0.255	**0.871**	−0.237	−0.127
Cl^{-}	−0.021	**0.812**	−0.235	−0.240
SO_4^{2-}	**0.602**	0.466	0.195	−0.115
F^{-}	−0.023	**0.722**	0.083	0.277
HCO_3^{-}	**0.635**	0.001	0.054	0.497
NO_3^{-}	**0.628**	−0.264	0.485	0.121
B	0.231	**0.761**	0.095	0.284
Br	0.188	**0.824**	−0.089	0.133
Cr	0.221	−0.203	**0.691**	0.325
Fe	0.004	−0.095	**−0.781**	0.314
Mn	−0.099	0.168	**−0.922**	−0.035
Ni	**0.763**	−0.228	−0.273	0.044
Sr	**0.645**	0.506	0.210	0.042
Zn	0.081	0.080	−0.041	**0.844**
Eigenvalue	4.612	3.975	1.921	1.227
Cumulative eigenvalue	4.612	8.587	10.508	11.735
Explained variance (%)	28.826	24.841	12.008	7.669
Cumulative % of variance	28.826	53.667	65.675	73.344

Significant loadings are in bold and underlined.

et al., 2004; Fernandes et al., 2008). Regarding this result, our explanation is that the types of chemical fertilizers that are being used in TCP area (e.g., calcium nitrate, magnesium nitrate, ammonium sulfate, etc.) also contain the major ions (Ca^{2+}, Mg^{2+}, SO_4^{2-}, etc.) that normally result from natural water–rock interaction processes. Significant correlation coefficients (at p-level < 0.05) between nitrate and major ions Ca (r = 0.52), Mg (r = 0.42), and SO_4 (r = 0.23) also support this association and offer an explanation for the superposition of the geogenic and anthropogenic factors in PC1. Similar findings were also obtained from recent studies conducted in various parts of the world, where major hydrochemical variables (i.e., Ca^{2+}, Na^{+}, SO_4^{2-}, and Cl^{-}) are associated with NO_3^{-} due to pollution mainly from anthropogenic (i.e., agricultural) sources (e.g., Aiuppa et al., 2003; Jayaprakash et al., 2008; Yammani et al., 2008; Koh et al., 2009). It can be said that PC1 is a prominent factor in TCP area that indicates the high vulnerability of the area to agricultural contaminants. This finding is likely to have important implications for the future management strategies of the basin (i.e., restriction on the use of certain types of fertilizers in some parts of the TCB). Sr is also well-known for its association with carbonates, where it can readily substitute for Ca in the limestone and dolomite. For instance, reported Sr concentrations of lower-middle Miocene Karaisalı formation (reefal limestone) range from 148 to 253 ppm (Büyükutku, 2009). The origin of Sr can also be attributed to sea spray and fertilizers used in this area (Kume et al., 2010), as well as dissolution of evaporitic series in Miocene–Pliocene formations (see FCM Class 4 Sr values in Table 4). The source of Ni is probably geogenic, since ultramafic (ophiolitic) rocks are common throughout area (Yaman, 1991; Şenol et al., 1998).

A map showing the spatial distribution of PC1 scores is presented in Fig. 6a, where high scores (i.e., values from 0.2 to 2.55) are generally observed at the northern parts of the study area, where FCM Class 1 waters prevail (see Fig. 5). Therefore, PC1 (or as it is called "water–rock interaction and nitrate contamination" factor) can be accepted as the main factor controlling the FCM Class 1 water chemistry. Most of the samples in FCM Class 1 can be regarded as recharge area waters due to dominance of Ca–Mg–HCO_3 water type (34% of

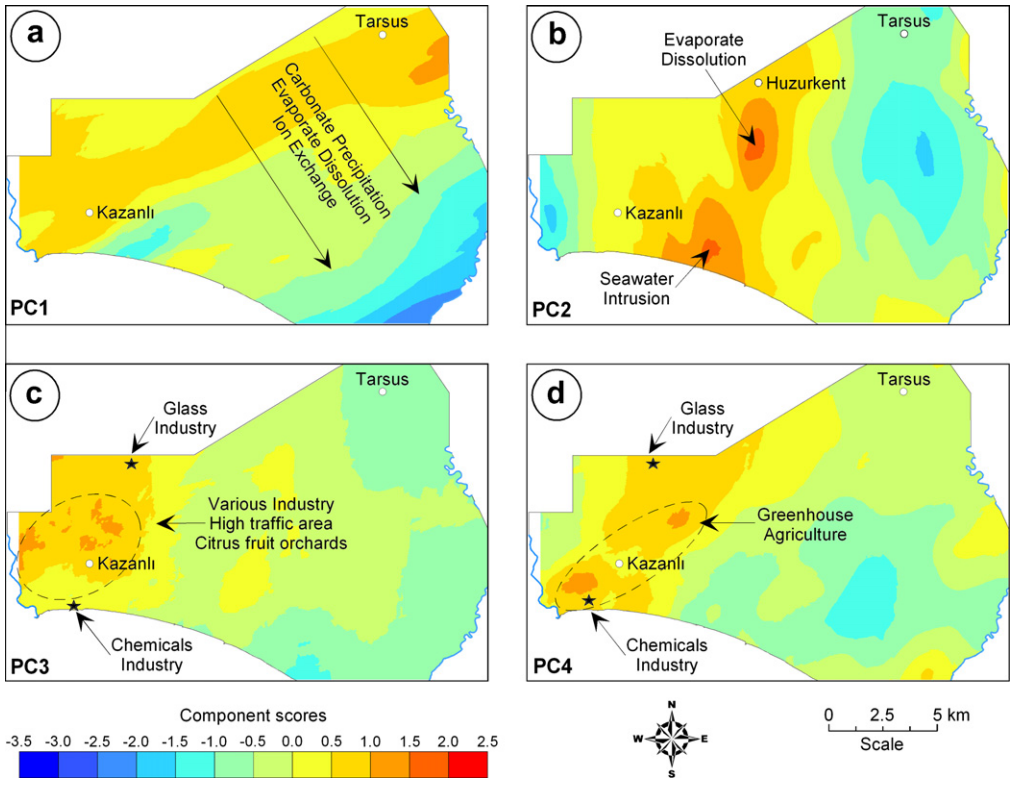

Fig. 6. Maps showing the spatial distribution of four PC scores obtained by principal components analysis of the groundwater samples: (a) PC1: Ca^{2+}, Mg^{2+}, SO_4^{2-}, HCO_3^{-}, NO_3^{-}, Ni, and Sr; (b) PC2: Na^{+}, Cl^{-}, F^{-}, B, and Br; (c) PC3: Cr, Fe, and Mn; and (d) PC4: Zn. Positive PC values indicate the areas most affected by the chemical process(es) described by each PC.

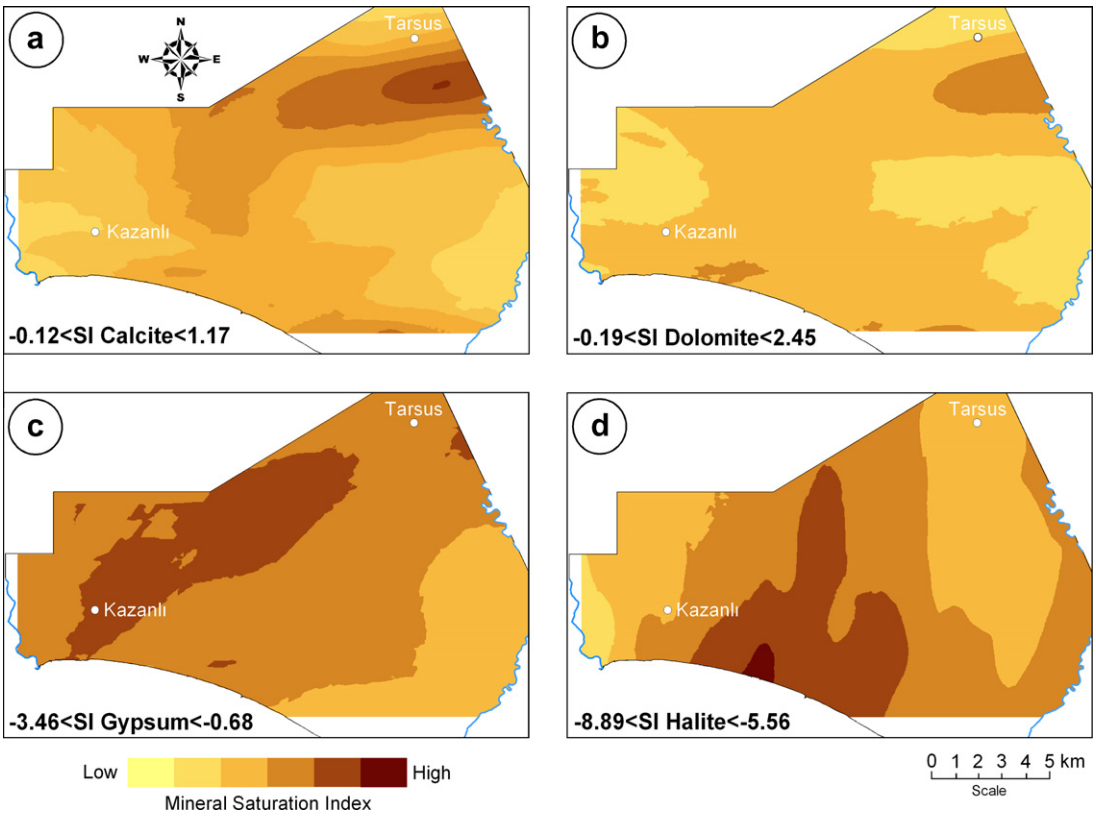

Fig. 7. Maps showing the spatial distribution of PHREEQC (Parkhurst and Appelo, 1999) calculated saturation indices (SI) for the four mineral phases: (a) calcite, (b) dolomite, (c) gypsum, and (d) halite.

the Class 1 waters). Presumably, flow through fracture network has been slow enough that calcite and dolomite equilibrium was achieved (Fig. 7a and b) before Class 1 waters enter the TCP basin. However, once they enter the fluvio-deltaic coastal aquifer, chemical character of Class 1 waters changes drastically. Along the groundwater flow path the concentrations of Ca^{2+} and Mg^{2+} ions decrease, as concentrations of Na^+, SO_4^{2-}, and Cl^- ions increase. This corresponds very well to the systematic decrease in PC1 scores (Fig. 6a) in NW–SE direction, suggesting that hydrochemical processes creating FCM Class 1 waters are decreasing in intensity along the groundwater flow path. In TCP, decrease in Ca^{2+}, Mg^{2+}, and HCO_3^- concentrations in FCM Class 1 waters can be explained by carbonate precipitation (e.g., calcite, dolomite, etc.):

$$Ca^{2+} + HCO_3^- = CaCO_3 + H^+ \quad (2)$$

$$Ca^{2+} + Mg^{2+} + 2HCO_3^- = CaMg(CO_3)_2 + 2H^+ \quad (3)$$

These reactions are thermodynamically favored and PHREEQC calculated saturation indices for both calcite (Fig. 7a) and dolomite (Fig. 7b) decrease along the groundwater flow path (calcite SI values decrease from 0.81 to 0.21 and dolomite SI values from 1.45 to 0.57). Except for a few samples, all groundwater samples from the TCP remain supersaturated with respect to calcite ($-0.12 < SI < 1.17$) and dolomite ($-0.19 < SI < 2.45$) along the flow path, where the lowest calcite and dolomite SI values occur near the lower reaches of the Deliçay and Tarsus rivers (Fig. 7a and b).

Apart from seawater intrusion, increase in SO_4^{2-} concentrations is only locally important in TCP and mostly confined to the area between Huzurkent and Adanalıoğlu settlements (shallow aquifer), where underlying Miocene–Pliocene formations known to contain thick layers of gypsum. Throughout the TCP, groundwater samples remain undersaturated with respect to gypsum ($-3.46 < SI < -0.68$) (Fig. 7c), which indicates that gypsum dissolution is favored in the aquifer, in accordance with the following reaction:

$$CaSO_4 \cdot 2H_2O = Ca^{2+} + SO_4^{2-} + 2H_2O \quad (4)$$

The highest gypsum SI values generally occur in the shallow aquifer overlying the Miocene–Pliocene formations, which is represented by Class 4 waters. Additionally, the high SO_4^{2-} concentration and its correlation with Ca ($r = 0.60$ at p-level = 0.00) indicate that the source is mainly gypsum (other sources include fertilizers/waste waters containing sulfate and seawater; see Table 2). However, carbonate precipitation or gypsum dissolution reactions alone cannot explain the increase in Na^+ and to a lesser extent Cl^- concentrations along the flow path. Considering that the aquifer has high smectitic clay content (20–67% in 0–150 cm of topsoil; unpublished data), there is probably an important contribution from the ion exchange reactions (Ca^{2+} and Mg^{2+} replacing Na^+ in clays). This also explains the decrease in Ca^{2+} and Mg^{2+} and the increase in Na^+ concentrations along the flow path (Domenico and Schwartz, 1997). Darbaş et al. (2008) have also reported high amounts of smectite in formations from the Miocene (average 28.6%) and Pliocene (average 56.8%) in the area. Ion exchange reactions are also called "natural water softening reactions" since Ca^{2+} and Mg^{2+} ions are removed from the water.

$$Ca^{2+}(\text{or } Mg^{2+}) + 2Na - \text{clay} = 2Na^+ + Ca(\text{or } Mg) - \text{clay} \quad (5)$$

The highest nitrate concentrations occur in FCM Class 1 and Class 4 waters with average values of 20.4 and 51.5 mg L^{-1}, respectively. The high average nitrate concentration of Class 4 waters is due to one extreme value (201.1 mg L^{-1}); however, when it is excluded the average value drops to 14.1 mg L^{-1}. The nitrate concentration in 10 groundwater samples is above the highest desirable limit defined for drinking water (45 mg L^{-1}). In TCP, the possible

sources for high nitrate concentrations in groundwater samples can be attributed to the use of fertilizers and domestic waste discharges. Low nitrate and oxygen concentrations in Class 2 and Class 3 waters (Table 3) indicate that it is naturally attenuated by denitrification in a weakly reducing environment. However, adverse effects such as increases in Fe and Mn concentrations (Table 4) follow the reduction reactions.

4.3.2. PC2 – Salinization by seawater intrusion and evaporite dissolution

PC2 explains 24.8% of the variance and is mainly related to elements Na^+, Cl^-, F^-, B, and Br (loadings ranging from 0.722 to 0.871). PC2 includes classical hydrochemical variables that indicate salinization processes. It is also worth to mention that in TCP the highest values of Na^+, Cl^-, B, and Br generally occur in the coastal areas intruded by the seawater (Class 2 and Class 3 waters in Fig. 5). In addition to that, high values of Ca^{2+}, Na^+, K^+, F^-, SO_4^{2-}, B, and Sr are mainly confined to the area between Huzurkent and Adanalıoğlu settlements (Class 4 waters), where evaporite dissolution (mainly gypsum) is the main process affecting the groundwater chemistry (Figs. 6b and 7c). Fig. 6b displays the distribution of the PC2 component scores in the study area, where the highest scores (i.e., values from 0.2 to 2.59) are generally observed at two localized areas at the southern parts of the Huzurkent and southeastern parts of the Kazanlı settlements. These hot spots correspond well to areas where FCM defined Class 2, Class 3, and Class 4 waters prevail (see Fig. 5). The increase in the salt content of TCP groundwater samples (i.e., aquifer salinization) could be accounted for mainly by two different mechanisms: (1) seawater intrusion (Class 2 and Class 3 waters) and (2) dissolution of evaporitic series from the Handere formation (Class 4 waters). Additionally, seawater trapped in the sediments or sea-spray probably contributes to the salinization of the groundwaters in the area. In TCP, groundwater samples remain undersaturated with respect to halite ($-8.89 < SI < -5.56$) and highest halite SI values occur in the areas of active seawater intrusion (Fig. 7d), where FCM Class 2 and Class 3 waters prevail (Fig. 5).

To evaluate the salinization by seawater intrusion, the seawater fraction (f_{sea}) of each groundwater sample was estimated (using Eq. (6)) based on chloride (Cl^-), since it is considered to be a conservative tracer (Appelo and Postma, 1994):

$$f_{sea} = \frac{m_{Cl^-(sample)} - m_{Cl^-(fresh)}}{m_{Cl^-(sea)} - m_{Cl^-(fresh)}} \quad (6)$$

For this calculation, representative Cl^- concentration of the freshwater end-member ($Cl^-_{(fresh)}$) was taken as the average value of the 36 groundwater samples from the recharge area. On the other hand, representative Cl^- concentration of the seawater end-member ($Cl^-_{(sea)}$) was taken as the average value of the two samples collected from the Mediterranean Sea (Table 2). The above calculation was carried out with an assumption that chloride is solely originated from seawater intrusion and sea spray. Fig. 8 shows the distribution of the seawater fraction (%) in groundwater samples and the areas affected by the active seawater intrusion. The aquifer contains a small portion of seawater in its southern part between Kazanlı and Kulak settlements. The calculated seawater

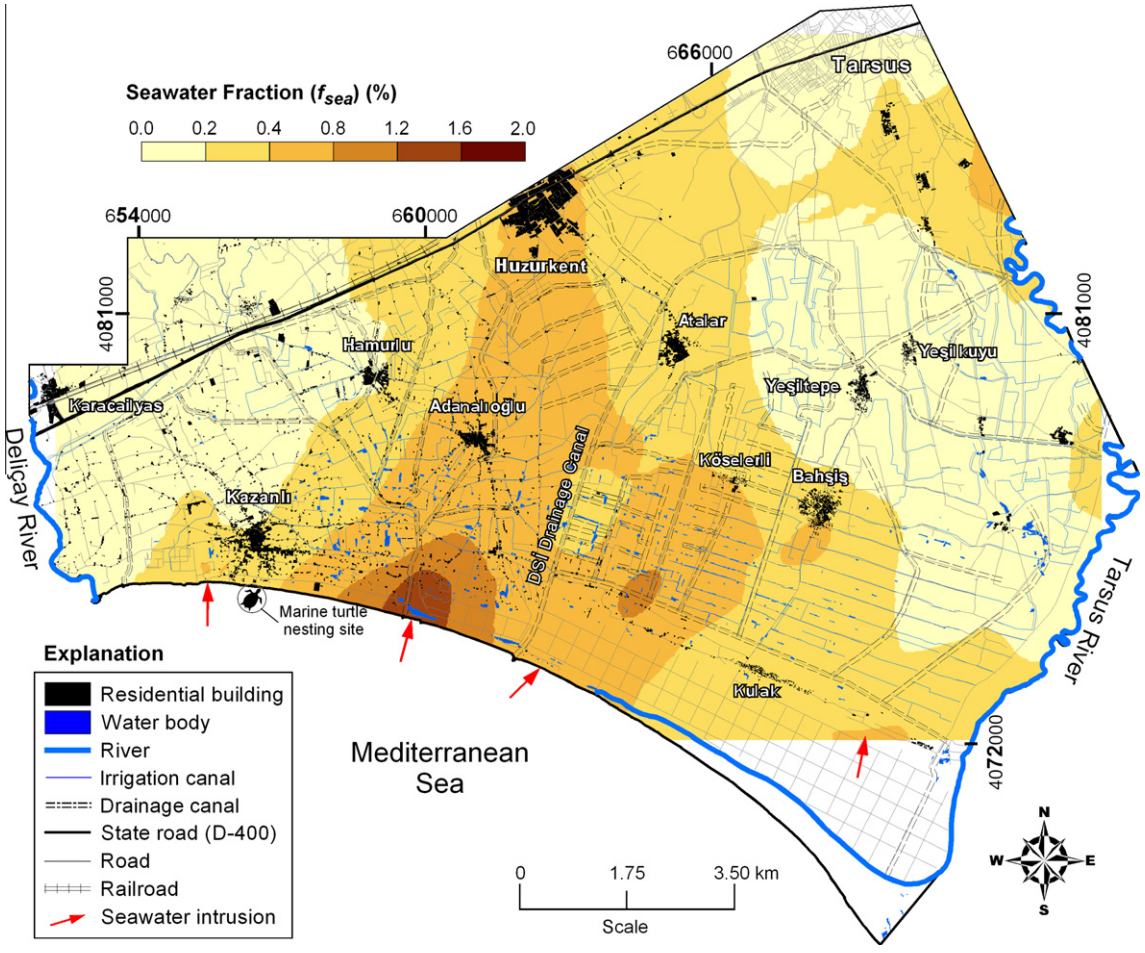

Fig. 8. Map showing the spatial distribution of seawater fractions (f_{sea}) of the groundwater samples.

fractions (f_{sea}) of the groundwater samples range from 0.09% to 0.82% for Class 2 waters, and it varies from 0.46% to 1.99% for Class 3 waters. Class 3 waters (EC = 1553 μS cm^{-1}) are almost twice more saline than Class 2 waters (EC = 966 μS cm^{-1}), where the difference in the salinities can be explained by proximity of Class 3 waters to the coastline and the sea (Fig. 5). In the present study, 7.8% of the coastal groundwater samples were found to contain chloride concentrations above 200 mg L^{-1} (max. value is 433 mg L^{-1}) suggesting that seawater intrusion has not reached alarming levels yet. This is probably because delta area has abundance of water, which effectively flushes the saltwater component while at the same time diluting it.

4.3.3. PC3 – Geogenic/anthropogenic Cr, Fe and Mn

The trace elements Cr, Fe, and Mn contribute most strongly to the third component (PC3) that explains 12% of the total variance (with a positive loading on Cr and negative loadings on Fe and Mn) (Table 5). In TCP area, high Cr concentrations generally occur where Fe and Mn concentrations are low and vice versa. Fig. 6c displays the distribution of the PC3 component scores in the study area, where the highest scores (i.e., values from 0.2 to 2.48) are generally observed in the area encircling settlements of Kazanlı, Karacailyas and Hamurlu. This part of the TCP is a high-traffic area due to the presence of various kinds of industries (e.g., soda-chromium chemicals and glass), petroleum hydrocarbon storage facilities and it is typified by the presence of dense citrus orchards and greenhouses (Fig. 1). In general, contamination of groundwater with heavy metals is attributed to anthropogenic sources; however, in TCP both geogenic and anthropogenic sources exist for the elements Cr, Fe and Mn. For instance, previous studies conducted in the area (Yaman, 1991; Koleli and Halisdemir, 2005) have reported very high concentrations of Cr in soil/rock samples, which are mostly attributed to the presence of chromium mineralizations in the Deliçay River watershed and to the presence of the soda-chromium chemicals industry near Kazanlı. However, chromium wastes (amounting 1.5×10^6 tons) stockpiled on alluvial soils by soda-chromium chemicals industry makes it a prime candidate for soil and groundwater pollution in the area. Interestingly, almost all of the groundwater samples having relatively high Cr concentrations (>10 μg L^{-1}) plot around the soda-chromium factory, where the highest measured Cr concentration was 62.8 μg L^{-1}. In high pH environments (e.g., pH > 6) the Cr is distributed among various hydroxyl complexes (e.g., $CrOH^{2+}$, $Cr(OH)_2^+$ and, $Cr(OH)_3^0$) (Domenico and Schwartz, 1997). In the seawater samples, Cr concentrations are even more pronounced, where concentrations reach up to 520.9 μg L^{-1} (Table 2). However, this value is much lower than the values reported previously (5400 μg L^{-1}) by some independent investigations carried out in Kazanlı area (Wolf, 2001). These high Cr values are possibly due to leakages from the waste retention basins of the soda-chromium industry located near the shore (Fig. 1). Chromium is listed in Appendix II of the protocol against pollution from land-based sources in the Mediterranean Sea under the "Barcelona Convention", which came in effect on February 12, 1978 and was last amended in 1995.

Heavy metals Fe and Mn; however, display a different spatial distribution when compared to Cr. The highest concentrations of Fe (348.1–2052 μg L^{-1}) and Mn (53–259.2 μg L^{-1}) are generally clustered around the Kazanlı and along the Mediterranean coastline, where dissolved oxygen (DO) concentrations are very low (DO < 1.5 mg L^{-1}). The natural weathering processes of the minerals are mainly responsible in release of Fe and Mn; however, their activities are mostly controlled by the redox level of groundwater. The high concentrations of these elements are likely due to reductive dissolution of Fe/Mn (hydr)oxides found in the aquifer sediments. In shallow groundwater flow systems and soils, the biogeochemical reactions mediated by autochthonous microorganisms have critical importance (Güler, 2009) and in low DO environments, they use a number of alternative electron acceptors to decompose organic material following the thermodynamic sequence: NO_3^- > Mn(IV) > Fe(III) > SO_4^{2-} > CO_2 to produce NH_4^+, N_2, Mn^{2+}, Fe^{2+}, H_2S, S^{2-}, S^0 and CH_4 (Ponnamperuma, 1972). In the TCP area, FCM Class 2 and Class 3 waters are the ones most affected by the anaerobic decomposition processes (redox reactions), which is evidenced by their very low NO_3^- concentrations due to denitrification (NO_3^- < 10 mg L^{-1}) and very high Fe/Mn concentrations due to reduction of Fe/Mn (hydr)oxides (see Tables 3 and 4). In general, it can be concluded that anomalous Fe and Mn concentrations are mainly restricted to narrow zones of highly depleted oxygen along the Mediterranean coastline; especially in waterlogged areas around greenhouses (see Fig. 1).

4.3.4. PC4 – Anthropogenic Zn pollution

Finally, the fourth component (PC4) is concerned solely with Zn (with a loading of 0.844) and represents 7.7% of the total variance (Table 5). Fig. 6d displays the distribution of the PC4 component scores in the study area, where the highest scores (i.e., values from 0.2 to 2.77) are generally observed around Kazanlı, Hamurlu and Adanalıoğlu settlements, where industrial activities and citrus orchards are widespread and greenhouse cultivation, as well as other modes of controlled environment cultivation is commonly practiced (see Fig. 1). It is known that nitrate fertilizers; such as calcium nitrate and potassium nitrate, are liberally applied to the agricultural soils of TCP. High Zn concentrations may be linked to use of this type of fertilizers, since the fertilizers used in this area are composite fertilizers containing up to 1% Zn as micronutrient (Güler et al., 2010). Gradually decreasing concentration of Zn away from these areas also confirms an agricultural source for this element.

5. Conclusions

Coastal delta environments are complex regarding geology, hydrogeology, biology and land use practices and present a unique challenge for sustainable use due to its structure (mostly constitute a complex/multilayer system). Tarsus coastal plain (TCP) lies in an economically and ecologically important area, where the sudden increase of population, rapid economic development, and intensive anthropogenic activities have collectively resulted in deterioration of groundwater resources (qualitatively and quantitatively) due to large amounts of pollution load received from a variety of point and diffuse sources and a very large increase in water demands over a period of three decades for agricultural, industrial, and domestic uses. In this semi-arid coastal region, the problems associated with water quality issues are of growing concern, since the increase of pollution in the area has lead to serious environmental consequences, which threaten the viability of the vulnerable ecosystems. Therefore, in TCP sustainable management of groundwater resources requires a good understanding of both groundwater circulation patterns and hydrologic/hydrochemical processes that affect their chemistry. The combination of techniques employed in this study (i.e., FCM, PCA, geostatistics, and GIS) provided an efficient way for analyzing a high-dimensional hydrochemical data set (193 cases and 24 variables) from the TCP area. The results of this study are promising and suggest that combination of these techniques can be successfully applied in characterization of environmental pollution and hydrogeochemical evolution along the groundwater flow paths in areas of complex natural and anthropogenic processes are in action.

In this study, FCM clustering method was used to create a spatially and hydrochemically coherent classification of water chemistry data. Using FCM method, four water classes were delineated

and prototypes representing each class were determined. The results suggest that fuzzy classification may better reflect the continuous nature of the processes underlying the generation of water chemistry variability in the study area. Additionally, multivariate analysis using PCA was applied to decipher underlying natural and anthropogenic processes creating these water classes. PCA results have shown that four major factors are responsible for the hydrochemical variability in the groundwater samples: (1) water–rock interaction and nitrate contamination; (2) salinization by seawater intrusion and evaporite dissolution; (3) geogenic/anthropogenic Cr, Fe, and Mn; and (4) anthropogenic Zn pollution. In general, the total ionic enrichment follows the groundwater flow path from the recharge areas to the discharge areas. In TCP area, anthropogenic activities responsible for the deterioration in quality of groundwater resources can be classified as: (1) excessive application fertilizers in agricultural areas; (2) discharge of various chemicals from the industrial facilities; and (3) overexploitation of the groundwater resources. To protect the vulnerable ecosystems and the vital groundwater sources from further deterioration, the government agencies should adopt strategies that could include: regulating the amount and type of synthetic chemicals (e.g., fertilizers, pesticides, etc.) applied to agricultural soils, monitoring of both groundwater pumping rates and waste disposal in industrial zones, and developing a groundwater monitoring network for assessment of the groundwater quality periodically.

Acknowledgements

The work reported in this paper has been performed as a part of project sponsored by DPT (State Planning Organization of Turkey) under the Grant Number DPT 2006 K 120770. Partial funding was also provided by the Mersin University Scientific Research Projects unit (Grant No: BAP-FBE-JM (MAK) 2007-2DR). This manuscript in draft was presented at the 7th International Symposium on Eastern Mediterranean Geology held in University of Çukurova, Adana, Turkey (18–22 October 2010). The authors would like to acknowledge the participants who made helpful suggestions at the presentation. The authors are also grateful to the editor Laurent Charlet and two anonymous reviewers for their useful suggestions.

References

Adams, S., Titus, R., Pietersen, K., Tredoux, G., Harris, C., 2001. Hydrochemical characteristics of aquifers near Sutherland in the Western Karoo, South Africa. J. Hydrol. 241, 91–103.

Aiuppa, A., Bellomo, S., Brusca, L., D'Alessandro, W., Federico, C., 2003. Natural and anthropogenic factors affecting groundwater quality of an active volcano (Mt. Etna, Italy). Appl. Geochem. 18, 863–882.

Appelo, C.A.J., Postma, D., 1994. Geochemistry, Groundwater and Pollution. A. A. Balkema, Brookfield.

Baltacı, F., Onur, A.K., Tahmiscioğlu, S., 2008. Water quality monitoring studies of Turkey with present and probable future constraints and opportunities. Desalination 226, 321–327.

Barbieri, P., Adami, G., Favretto, A., Lutman, A., Avoscan, W., Reisenhofer, E., 2001. Robust cluster analysis for detecting physico-chemical typologies of freshwater from wells of the plain of Friuli (northeastern Italy). Anal. Chim. Acta. 440, 161–170.

Bezdek, J.C., 1981. Pattern Recognition with Fuzzy Objective Function Algorithms. Plenum Press, New York.

Bezdek, J.C., Ehrlich, R., Full, W., 1984. FCM: the fuzzy *c*-means clustering algorithm. Comput. Geosci. 10, 191–203.

Bezdek, J.C., Keller, J.M., Krishnapuram, R., Pal, N.R., 1999. Fuzzy Models and Algorithms for Pattern Recognition and Image Processing. Kluwer Academic Publishers, Boston.

Burton-Ferguson, R., Aksu, A.E., Calon, T.J., Hall, J., 2005. Seismic stratigraphy and structural evolution of the Adana Basin, eastern Mediterranean. Mar. Geol. 221, 189–222.

Büyükutku, A.G., 2009. Reservoir properties of Karaisalı formation in the Adana Basin, Southern Turkey. J. Petrol. Sci. Eng. 65, 33–44.

Canbolat, A.F., 2004. A review of sea turtle nesting activity along the Mediterranean coast of Turkey. Biol. Conserv. 116, 81–91.

Cattell, R.B., 1966. The scree test for the number of factors. Multivar. Behav. Res. 1, 245–276.

Closs, L.G., Nichol, I., 1975. The role of factor and regression analysis in the interpretation of geochemical reconnaissance data. Can. J. Earth Sci. 12, 1316–1330.

Costello, A.B., Osborne, J.W., 2005. Best practices in exploratory factor analysis: four recommendations for getting the most from your analysis. Pract. Assess. Res. Eval. 10, 1–9.

Çelik, A., Kaska, Y., Bağ, H., Aureggi, M., Semiz, G., Kartal, A.A., Elçi, L., 2006. Heavy metal monitoring around the nesting environment of green sea turtles in Turkey. Water Air Soil Pollut. 169, 67–79.

Dalton, M.G., Upchurch, S.B., 1978. Interpretation of hydrochemical facies by factor analysis. Ground Water 16, 228–233.

Darbaş, G., Nazik, A., Temel, A., Gürbüz, K., 2008. A paleoenvironmental test of the Messinian Salinity Crisis using Miocene–Pliocene clays in the Adana Basin, Southern Turkey. Appl. Clay Sci. 40, 108–118.

Davis, J.C., 1986. Statistics and Data Analysis in Geology, second ed. John Wiley and Sons, Inc., New York.

Demirel, Z., 2004. The history and evaluation of saltwater intrusion into a coastal aquifer in Mersin, Turkey. J. Environ. Manage. 70, 275–282.

Domenico, P.A., Schwartz, F.W., 1997. Physical and Chemical Hydrogeology, second ed. John Wiley & Sons Inc., New York.

DSİ, 1978. Mersin, Berdan ve Efrenk Ovaları Hidrojeolojik Etüd Raporu. Ankara, Turkey.

Dunn, J.C., 1974. A fuzzy relative ISODATA process and its use in detecting compact well-separated clusters. J. Cybern. 3, 32–57.

ESRI, 2009. ArcGIS version 9.3. 380 New York Street, Redlands, CA 92373-8100 USA.

Fang, J.H., Chen, H.C., 1990. Uncertainties are better handled by Fuzzy arithmetic. AAPG Bull. 74, 1128–1233.

Fant, C.E., Reddish, M.G., 2003. A Guide to Biblical Sites in Greece and Turkey. Oxford University Press, New York.

Fernandes, P.G., Carreira, P., da Silva, M.O., 2008. Anthropogenic sources of contamination recognition – Sines coastal aquifer (SW Portugal). J. Geochem. Explor. 98, 1–14.

Freeze, R.A., Cherry, J.A., 1979. Groundwater. Prentice-Hall, Englewood Cliffs, New Jersey.

Goldman, H., 1950. Excavations at Gözlü Kule, Tarsus, vol. I: The Hellenistic and Roman Periods. Princeton University Press, Princeton, New Jersey.

Goldman, H., 1956. Excavations at Gözlü Kule, Tarsus, vol. II: From the Neolithic through the Bronz Age. Princeton University Press, Princeton, New Jersey.

Göney, S., 1976. Adana Ovaları I. İstanbul Üniversitesi Yayın No: 2162, Coğrafya Enstitüsü Yayın No: 88, İstanbul.

Gül, M., 2007. Effects of antecedent topography on reefal carbonate deposition: Early-Middle Miocene of the Adana Basin, S Turkey. J. Asian Earth Sci. 31, 18–34.

Güler, C., 2009. Site characterization and monitoring of natural attenuation indicator parameters in a fuel contaminated coastal aquifer: Karaduvar (Mersin, SE Turkey). Environ. Earth Sci. 59, 631–643.

Güler, C., Alpaslan, M., Kurt, M.A., Temel, A., 2010. Deciphering factors controlling trace element distribution in the soils of Karaduvar industrial-agricultural area (Mersin, SE Turkey). Environ. Earth Sci. 60, 203–218.

Güler, C., Thyne, G.D., 2004. Delineation of hydrochemical facies distribution in a regional groundwater system by means of fuzzy *c*-means clustering. Water Resour. Res. 40 (Article No. W12503), 1–11.

Güler, C., Thyne, G.D., McCray, J.E., Turner, A.K., 2002. Evaluation of graphical and multivariate statistical methods for classification of water chemistry data. Hydrogeol. J. 10, 455–474.

Gürbüz, K., 1999. An example of river course changes on a delta plain: Seyhan Delta (Çukurova plain, southern Turkey). Geol. J. 34, 211–222.

Gürbüz, K., 2003. Berdan Nehri'nin Kuvaterner'deki evrimi ve Tarsus'un tarihçesine jeolojik bir yaklaşım. Kuvaterner Çalıştayı IV. İTÜ Avrasya Yer Bilimleri Enstitüsü, 79–83.

Gürses, M.K., 1995. *Eucalyptus camaldulensis*'in yetişme ortamı istekleri. DOA Dergisi 1, 1–6.

Hancock, P.J., Boulton, A.J., Humphreys, W.F., 2005. Aquifers and hyporheic zones: towards an ecological understanding of groundwater. Hydrogeol. J. 13, 98–111.

Helena, B., Pardo, R., Vega, M., Barrado, E., Fernandez, J.M., Fernandez, L., 2000. Temporal evolution of ground water composition in an alluvial aquifer (Pisuerga River, Spain) by principal component analysis. Water Res. 34, 807–816.

Hill, T., Lewicki, P., 2007. STATISTICS Methods and Applications. StatSoft, Tulsa, OK.

Höppner, F., 2002. Speeding up Fuzzy *c*-Means: using a hierarchical data organization to control the precision of membership calculation. Fuzzy Set. Syst. 128, 365–378.

IUCN, 2007. IUCN Red List of Threatened Species. <http://www.iucnredlist.org> (accessed 10.01.08).

Jayaprakash, M., Giridharan, L., Venugopal, T., Kumar, S.P.K., Periakali, P., 2008. Characterization and evaluation of the factors affecting the geochemistry of groundwater in Neyveli, Tamil Nadu. India. Environ. Geol. 54, 855–867.

Kafalı Yılmaz, F., 2008. Adana Ovaları'nda İklim-Tarım İlişkisi ve Tarım Politikalarının Yansıması. A.K.Ü. Yayın No: 70, Afyonkarahisar.

Kaiser, H.F., 1960. The application of electronic computers to factor analysis. Educ. Psychol. Meas. 20, 141–151.

Karayakar, F., Erdem, C., Cıcık, B., 2007. Seasonal variation in copper, zinc, chromium, lead and cadmium levels in Hepatopancreas, gill and muscle tissues of the mussel *Brachidontes pharaonis* Fischer, collected along the Mersin coast, Turkey. Bull. Environ. Contam. Toxicol. 79, 350–355.

Kaska, Y., Çelik, A., Bağ, H., Aureggi, M., Özel, K., Elçi, A., Kaska, A., Elçi, L., 2004. Heavy metal monitoring in stranded sea turtles along the Mediterranean coast of Turkey. Fresen. Environ. Bull. 13, 769–776.

Koh, D.-C., Chae, G.-T., Yoon, Y.-Y., Kang, B.-R., Koh, G.-W., Park, K.-H., 2009. Baseline geochemical characteristics of groundwater in the mountainous area of Jeju Island, South Korea: implications for degree of mineralization and nitrate contamination. J. Hydrol. 376, 81–93.
Koleli, N., Halisdemir, B., 2005. Distribution of chromium, cadmium, nickel and lead in agricultural soils collected from Kazanlı-Mersin, Turkey. Int. J. Environ. Pollut. 23, 409–416.
Kumbur, H., Özsoy, H.D., Özer, Z., 2008. Mersin ilinde tarımsal alanlarda kullanılan kimyasalların su kalitesi üzerine etkilerinin belirlenmesi. Ekoloji 17, 54–58.
Kume, T., Akca, E., Nakano, T., Pagano, T., Kapur, S., Watanabe, T., 2010. Seasonal changes of fertilizer impacts on agricultural drainage in a salinized area in Adana, Turkey. Sci. Tot. Environ. 408, 3319–3326.
Lucieer, V., Lucieer, A., 2009. Fuzzy clustering for seafloor classification. Mar. Geol. 264, 230–241.
Mahlknecht, J., Steinich, B., de León, I.N., 2004. Groundwater chemistry and mass transfers in the Independence aquifer, central Mexico, by using multivariate statistics and mass-balance models. Environ. Geol. 45, 781–795.
McBratney, A.B., Moore, A.W., 1985. Application of fuzzy sets to climatic classification. Agr. Forest Meteorol. 35, 165–185.
MEDASSET, 2001. Conservation Priority for the Green Turtle (*Chelonia mydas*) in Turkey (2001). <http://www.medasset.org/cms/index.php?option=com_ docman&task=doc_download&gid=83&Itemid=85&lang=el> (accessed 10.12.09).
MEDASSET, 2009. Kazanli, Turkey. <http://www.medasset.org/cms/index.php?option=com_ content&view=article&id =46%3Aturkey2&catid= 6%3Aactivities&Itemid=39&lang=en> (accessed 10.12.09).
Ministry of Environment and Forestry, 2008. 2007 yılı Mersin İl Çevre Durum Raporu. <http://www.mersin-cevreorman.gov.tr/mersinicd2007.pdf> (accessed 20.09.08).
Ministry of Environment and Forestry, 2009. National climate change strategy: Republic of Turkey. <http://www.undp.org.tr/energEnvirDocs/Ingilizce%20-%20Strateji%20Belgesi.pdf> (accessed 31.12.09).
Moore, W.S., 1999. The subterranean estuary: a reaction zone of ground water and sea water. Mar. Chem. 65, 111–125.
Murgai, R., Ali, M., Byerlee, D., 2001. Productivity growth and sustainability in post-green revolution agriculture: the case for the Indian and Pakistan Punjabs. World Bank Res. Obser. 16, 199–218.
Öner, E., Hocaoğlu, B., Uncu, L., 2005. Tarsus ovasının jeomorfolojik gelişimi ve Gözlükule Höyüğü. Türkiye Kuvaterner Sempozyumu (TURQUA-V). İTÜ Avrasya Yer Bilimleri Enstitüsü 2-5 June 2005, 82–89.
Öztürk, H.K., 2004. Present status and future prospects of hydroelectric energy in Turkey. Energ. Source. Part A 26, 829–840.
Parkhurst, D.L., Appelo, C.A.J., 1999. User's guide to PHREEQC (Version 2) – a computer program for speciation, batch-reaction, one-dimensional transport, and inverse geochemical calculations: US Geological Survey Water-Resources Investigations Report 99-4259.
Ponnamperuma, F.N., 1972. The chemistry of submerged soils. Adv. Agron. 24, 29–96.
R Development Core Team, 2007. R (version 2.5.1): A Language and Environment for Statistical Computing. R Foundation for Statistical Computing, Vienna, Austria.
Reimann, C., Filzmoser, P., Garrett, R.G., 2005. Background and threshold: critical comparison of methods of determination. Sci. Tot. Environ. 346, 1–16.
Rother, L., 1971. Die Städte der Çukurova: Adana-Mersin-Tarsus, Tübingen.
Roubens, M., 1982. Fuzzy clustering algorithms and their cluster validity. Eur. J. Oper. Res. 10, 294–301.
Sandal, E.K., Gürbüz, M., 2003. Mersin şehrinin mekansal gelişimi ve çevresindeki tarım alanlarının amaç dışı kullanımı. Coğrafi Bilimler Dergisi 1, 117–130.
Schmidt, G., 1961. VII. Adana Petrol Bölgesinin Stratigrafik Nomenklatürü. Petrol Dergisi 6, 47–63.
Şenol, M., Şahin, Ş., Duman, T.Y., 1998. Adana-Mersin Dolayının Jeoloji Etüd Raporu. M.T.A., Ankara.
Thyne, G., Güler, C., Poeter, E., 2004. Sequential analysis of hydrochemical data for watershed characterization. Ground Water 42, 711–723.
Uslu, T., 1989. Geographical Information on Turkish Coastal Dunes, European Union for Dune Conservation and Coastal Management Publication, Leiden.
Ünlügenç, U.C., 1986. Kızıldağ-Yayla (Adana) dolayının jeolojik incelemesi. Çukurova Üniversitesi Fen Bilimleri Enstitüsü, Master's Thesis, Adana.
Wolf, U., 2001. Kazanlı Environmental Pollution in March 2001: Report on the Chemical Analysis of Samples – Preliminary Results of a Rapid Assessment, Unpublished Report, 10 p.
Xie, X.L., Beni, G., 1991. A validity measure for fuzzy clustering. IEEE Trans. Pattern Anal. 13, 841–847.
Yaman, S., 1991. Mersin ofiyolitinin jeolojisi ve metallojenisi. Ahmet Acar Jeoloji Sempozyumu Bildirileri 225, 267.
Yammani, S.R., Reddy, T.V.K., Reddy, M.R.K., 2008. Identification of influencing factors for groundwater quality variation using multivariate analysis. Environ. Geol. 55, 9–16.
Yetiş, C., Demirkol, C., 1986. Adana Baseni Batı Kesiminin Detay Jeoloji Etüdü. MTA Raporu. Rapor No. 8037, 187 p.
Yetiş, C., Kelling, G., Gökçen, S.L., Baroz, F., 1995. A revised stratigraphic framework for later Cenozoic sequences in the northeastern Mediterranean region. Geol. Rundsch. 84, 794–812.
Yılmaz, A., Salihoğlu, İ., Latif, M.A., Yemenicioğlu, S., 1998. Oceanographic investigations related to a sewerage outfall in Mersin Bay. Turkish J. Eng. Environ. Sci. 22, 155–166.
Yılmaz, K.T., 1998. Ecological diversity of the Eastern Mediterranean region of Turkey and its conservation. Biodivers. Conserv. 7, 87–96.
Zadeh, L.A., 1965. Fuzzy sets. Inform. Control 8, 338–353.
Zoroğlu, L., 1995. Tarsus, Tarihi ve Tarihsel Anıtları, Kemal Matbaası, Adana.